# The effect of NETO2 on synaptosomal kainate receptor subunit levels in fear-related brain regions

Master's thesis

Emilie Rydgren

University of Helsinki

Faculty of Biological and Environmental Sciences

Molecular and Integrative Biosciences Research Programme

Biology programme / Physiology and Neuroscience

## Abstract


| Tiedekunta – Fakultet – Faculty | Laitos – Institution– Department |
|---|---|
| Faculty of Biological and Environmental Sciences | Molecular and Integrative Biosciences Research Program (previously Department of Biosciences) |

Tekijä – Författare – Author

Emilie Rydgren


Työn nimi – Arbetets titel – Title

The effect of NETO2 on synaptosomal kainate receptor subunit levels in fear-related brain regions

Oppiaine – Läroämne – Subject

Physiology and Neuroscience

| Työn laji – Arbetets art – Level | Aika – Datum – Month and year | Sivumäärä – Sidoantal – Number of pages |
|---|---|---|
| Master's thesis | June 2018 | 53 |


Tiivistelmä – Referat – Abstract

Kainate receptors (KARs) are glutamate receptors that modulate neurotransmission and neuronal excitability. They assemble from five subunits (GRIK1-5 or GluK1-5) present at both pre- and postsynaptic membranes. KAR function is regulated by neuropilin and tolloid-like (NETO) proteins, which also regulate postsynaptic GRIK2 abundance. Some KAR subunit gene variants associate with psychiatric disorders. Moreover, *Grik1, Grik2* and *Grik4* knock-out (KO) mice display changes in anxiety- and fear-related behaviours.

In previous work, *Neto2* KO mice expressed higher fear and impaired fear extinction in the fear conditioning paradigm. We hypothesised that this phenotype could be due to reduced KAR subunit abundance in fear-related brain regions, i.e. ventral hippocampus, amygdala and medial prefrontal cortex (mPFC). We specifically investigated GRIK2/3 and GRIK5 levels in the subcellular synaptosomal (SYN) fraction using western blot.

We did not observe any difference between genotypes in any of the brain regions. However, our statistical power may have been insufficient, particularly for amygdala and mPFC. Also, an effect on synaptic KAR subunit abundance might be specific to either pre- or postsynaptic compartment, and thus more difficult to detect in SYN fractions. Alternatively, NETO2 absence may affect KAR actions instead of their subunit levels in fear-related brain regions, which could be examined through electrophysiological recordings. Ultimately, unravelling how a molecular system without NETO2 gives rise to fear behaviour in mice may lead to a better understanding of fear-related disorders in human and to new therapeutic strategies.



Avainsanat – Nyckelord – Keywords

Kainate receptor, synapse, NETO2, psychiatric disorders, anxiety, fear conditioning, cerebellum, ventral hippocampus, amygdala, medial prefrontal cortex, subcellular fractionation, western blot

Ohjaaja tai ohjaajat – Handledare – Supervisor or supervisors

Iiris Hovatta and Marie Mennesson

Säilytyspaikka – Förvaringställe – Where deposited

Molecular and Integrative Biosciences Research Program

Muita tietoja – Övriga uppgifter – Additional information

| Tiedekunta – Fakultet – Faculty | Laitos – Institution– Department |
|---|---|
| Bio- och miljövetenskapliga fakulteten | Forskningsprogrammet för molekylära och integrativa biovetenskaper (förut Biovetenskapliga institutionen) |

Tekijä – Författare – Author
Emilie Rydgren

Työn nimi – Arbetets titel – Title
Effekten av NETO2 på nivån synaptosomala kainat receptor subenheter i rädslo-relaterade hjärnområden

Oppiaine – Läroämne – Subject
Fysiologi och neurovetenskaper

| Työn laji – Arbetets art – Level | Aika – Datum – Month and year | Sivumäärä – Sidoantal – Number of pages |
|---|---|---|
| Pro gradu | Juni 2018 | 53 |

Tiivistelmä – Referat – Abstract

Kainat receptorer (KARs) är glutamatreceptorer som modulerar nervimpulsöverföring och nervcellers retbarhet. De sammansätts utav fem subenheter (GRIK1-5 eller GluK1-5) som finns i både pre- och postsynaptiska membran. KARs funktion regleras av neuropilin och tolloidliknande (NETO) proteiner som också reglerar den postsynaptiska nivån GRIK2. Vissa varianter av KAR subenhetsgener associerar med psykiska störningar. Dessutom uppvisar *Grik1, Grik2* och *Grik4* knock-out (KO) möss förändringar i ångest- och rädslo-relaterade beteenden.

I tidigare arbete uttryckte *Neto2* KO möss högre rädsla och försämrad utrotning av rädsla i rädslo-konditionerings paradigmet. Vi hypotetiserade att denna fenotyp skulle kunna bero på minskad nivå KAR subenheter i rädslo-relaterade hjärnområden, d.v.s. ventrala hippocampus, amygdala och mediala prefrontala hjärnbarken (mPFC). Vi undersökte specifikt nivån GRIK2/3 och GRIK5 i den subcellulära synaptosomala (SYN) fraktionen med western blot.

Vi observerade ingen skillnad mellan genotyperna i någon av hjärnområdena. Vår statistiska kraft kan däremot ha varit otillräcklig, särskilt för amygdala och mPFC. En effekt på KAR subenheters synaptiska nivå kan också vara specifik för antingen pre- eller postsynaptiska regionen och således svårare att upptäcka i SYN fraktioner. Alternativt påverkar NETO2 frånvaro KARs verksamhet istället för deras nivå subenheter i rädslo-relaterade hjärnområden, som kan undersökas genom elektrofysiologiska mätningar. Att lösa hur ett molekylärt system utan NETO2 ger upphov till rädslo-beteende hos möss kan slutligen leda till en bättre förståelse för rädslo-relaterade störningar hos människan och till nya behandlingsmetoder.

Avainsanat – Nyckelord – Keywords
Kainat receptorer, synaps, NETO2, psykiska störningar, ängsla/ångest, rädslo-konditionering, cerebellum, ventrala hippocampus, amygdala, mediala prefrontala hjärnbarken, subcellulär fraktionering, western blot

Ohjaaja tai ohjaajat – Handledare – Supervisor or supervisors
Iiris Hovatta och Marie Mennesson

Säilytyspaikka – Förvaringställe – Where deposited
Forskningsprogrammet för molekylära och integrativa biovetenskaper

Muita tietoja – Övriga uppgifter – Additional information

## Acknowledgements

I wish to express my sincerest gratitude to my thesis project supervisors Iiris Hovatta and Marie Mennesson. I cannot thank you enough for your excellent guidance, commendable patience, invaluable feedback and your tireless dedication to supporting and advising me throughout my learning process of this thesis. I learned a lot from you and I could not have asked for more excellent supervisors.

I also want to thank the personnel of the Biomolecular Complex Purification (Biocomplex) for their equipment, assistance and expertise in ultracentrifugations. I thank the Neuroscience Center for letting me use their GBOX and VICTOR machines and the Laboratory Animal Centre for maintaining the mice.

A big thank you also goes to Ari Rouhiainen for his advice and expertise in western blot and I want to thank all the Neurogenomics lab members for their encouragements and friendship.

I also thank my friends and family for helping me unwind with good times and a lot of laughter.

Finally, I want to thank my admirable fiancé for his endless love, encouragement and support, for cheering me on during difficult times, for celebrating my successes and for helping me overcome my fears. I am lucky to have you by my side.

Thank you all.

# Table of contents

## Abbreviations

| | |
|---|---|
| AB | Antibody |
| ACTB | Actin, beta |
| Amg | Amygdala |
| AMPA | α-amino-3-hydroxy-5-methyl-4-isoxazolepropionic acid |
| BD | Bipolar disorder |
| BLA | Basolateral amygdala |
| BSA | Bovine serum albumin |
| cbr | Calibrator sample |
| CB1 | Cannabinoid receptor 1 |
| CCK | Cholecystokinin |
| Ceb | Cerebellum |
| Cing | Cingulate cortex area |

| | |
|---|---|
| CS | Conditioned stimulus |
| CUB | Complement C1r/C1s, Uegf and Bmp1 |
| dHPC | Dorsal hippocampus |
| DKO | Double-knockout |
| DLG4 | Discs large MAGUK scaffold protein 4 (also known as PSD-95) |
| DTT | Dithiothreitol |
| GABA | γ-aminobutyric acid |
| GAD | Generalised anxiety disorder |
| GRIK1-5 | Glutamate receptor, ionotropic, kainate 1-5 (also known as GluK1-5) |
| GRIP | Glutamate receptor binding protein |
| H | Homogenate |
| HPC | Hippocampus |
| HRP | Horse radish peroxide |
| Hyp | Hypothalamus |
| IL | Infralimbic area |
| IVC | Individually ventilated cage |
| KAR | Kainate receptor |
| KCC2 | $K^+$-$Cl^-$ cotransporter |
| KO | Knock-out |
| Lad | Prestained Protein Ladder |
| LD | Loading dye containing a reducing agent |
| LDLa | Low-density lipoprotein class A |
| MPB | Myelin basic protein |

| | |
|---|---|
| mPFC | Medial prefrontal cortex |
| NETO1/2 | Neuropilin and tolloid-like 1 and 2 |
| NMDA | N-methyl-D-aspartate |
| OCD | Obsessive compulsory disorder |
| Olf | Olfactory bulb |
| PDZ | Postsynaptic density protein-95, drosophila disc large tumour suppressor, and zonula occludens-1 protein |
| PL | Prelimbic area |
| PSD | Postsynaptic density |
| PTSD | Posttraumatic stress disorder |
| PV | Parvalbumin |
| P1-4 | Pellet 1-4 |
| SDS | Sodium dodecyl sulfate |
| SOM | Somatostatin |
| SYN | Synaptosomal |
| SYP | Synaptophysin |
| S1-3 | Supernatant 1-3 |
| TBS(-T) | Tris-buffered saline (with 0.1% TWEEN® 20) |
| TGS | Tris/Glycine/SDS |
| Tha | Thalamus |
| US | Unconditioned stimulus |
| vHPC | Ventral hippocampus |
| WT | Wild-type |

# 1. Introduction

## 1.1. Fear and anxiety

Fear has evolutionarily contributed to the survival of our species. It is the emotional response to a real or perceived imminent threat that usually triggers the autonomic fight-or-flight response and escape behaviours in order to cope with the adverse or unexpected situation (American Psychiatric Association 2016). Anxiety, on the other hand, is a sustained fear in the anticipation of a future threat (American Psychiatric Association 2016). When anxiety becomes excessive and chronic, it can be a life altering condition. Anxiety- and fear-related disorders, including generalised anxiety disorder (GAD), panic disorder, phobias, posttraumatic stress disorder (PTSD) and obsessive compulsory disorder (OCD), are the most frequent mental disorders in the EU population (Wittchen *et al.* 2011). The excessive fear and/or anxiety underlying these disorders are often stress-induced (American Psychiatric Association 2016) and may develop through associative fear learning (Maren & Holmes 2016). Thus, treatment of these disorders includes extinction learning of the acquired fear through behavioural therapies, such as exposure therapy (Maren & Holmes 2016). Understanding the excessive fear and its extinction on a biological level can reveal more specific therapeutic targets in order to correct the maladapted fear-processing network instead of just treating the symptoms.

Hippocampus (HPC), amygdala and medial prefrontal cortex (mPFC) are known to play an important role in anxiety regulation, and in fear expression and memory in human and rodent (Maren & Holmes 2016) (Figure 1). The HPC is important for the representation of the context of fearful memories and is known to be implicated in fear disturbance disorders such as PTSD (Maren & Holmes 2016). Notably, the dorsal (dHPC) and ventral part (vHPC) (Figure 1) of the HPC play different roles in the brain. The dorsal part is important for spatial cues and contextual memories (i.e. memory of the environment) and the ventral part is crucial for emotionally connoted memory such as fear memory (Strange *et al.* 2014). Amygdala is the centre of emotional learning, collecting sensory information, and is thus crucial for the organism's response to fearful

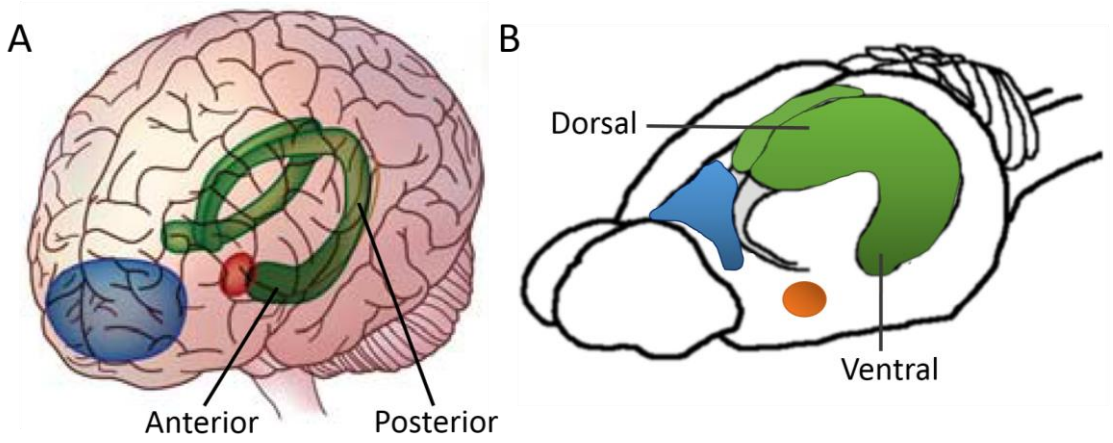


**Figure 1. Fear-related brain regions in human and mouse. A & B** Hippocampus is coloured green, amygdala is coloured orange, and (**A**) prefrontal cortex and (**B**) medial prefrontal cortex are coloured blue. The dorsal-intermediate rodent hippocampus is homologous with the posterior human hippocampus and the ventral rodent hippocampus is homologous with the anterior human hippocampus. **A.** Human brain figure adapted from Maren & Holmes (2016) and **B.** mouse brain figure modified from Spijker & Li (2011).

situations, extensively modelled by the fear conditioning paradigm (Maren & Holmes 2016) (Figure 2). Amygdala clearly initiates fear conditioning and extinction (Maren & Holmes 2016, Marek *et al.* 2018). It is also involved in generating freezing behaviour (total immobility apart from breathing), which is a natural response by rodents to fearful situations, through an amygdala-midbrain-medullary circuit (Tovote *et al.* 2016). Finally, mPFC connects to both HPC and amygdala, and plays an important role in fear

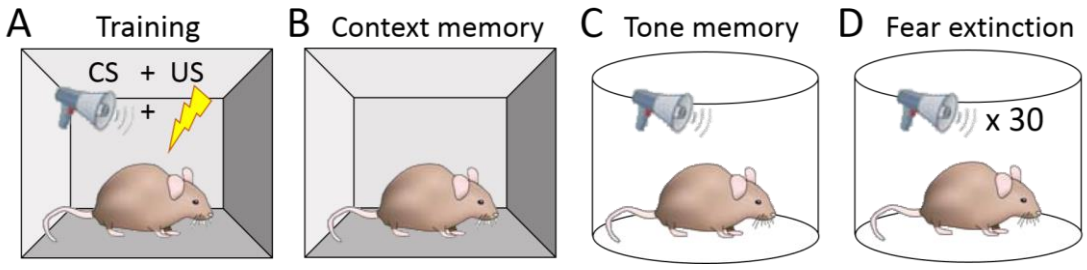


**Figure 2**. **Fear conditioning paradigm with shock and tone cue. A.** A mouse is trained to associate a naturally fear-inducing footshock stimulus (unconditioned stimulus, UC) to a neutral tone stimulus (conditioned stimulus, CS). Fear expression, as measured by freezing behaviour, to **B.** physical context and to **C.** tone cue (i.e. CS) are tested separately. **D.** Fear response extinction, i.e. extinction of the previously acquired fear, is tested with multiple tone cue presentations. Figure mouse and megaphone adapted from Maren & Holmes (2016).

conditioning and extinction (Maren & Holmes, 2016). The reigning view is that the prelimbic area (PL) drives expression of conditioned fear, such as freezing behaviour, while the infralimbic area (IL) is involved in generating extinction memories (Maren & Holmes 2016, Marek *et al.* 2018). Neuronal projections from the basolateral nucleus (BLA) of the amygdala to these two areas are recruited for fear conditioning and extinction (Maren & Holmes, 2016).

### 1.2. Kainate receptors

Kainate receptors (KARs) are ionotropic glutamate receptors assembled from a combination of subunits GRIK1-GRIK5 into tetramers (Figure 3). GRIK1-GRIK3 are low-affinity subunits that can form homomers, while GRIK4 and GRIK5 are high-affinity subunits that make functional receptors only when combined with low-affinity subunits (Evans *et al.* 2017). KAR subunits have a very distinct distribution in the brain, restricted to specific neurons and synapses (Straub *et al*. 2011, Tomita & Castillo 2012, Sheng *et al.* 2017). Nevertheless, *Grik1-5* genes are expressed throughout the brain (Allen Brain Institute 2018, Watanabe-Iida *et al.* 2016). KARs are found at both pre- and postsynaptic membranes (Lerma J. 2003, Isaac *et al.* 2004, Sheng *et al.* 2017) (Figure 3). They modulate transmitter release presynaptically at both excitatory and inhibitory synapses (Lerma J. 2003, Zhou M. 2017) (Figure 3) and they also modulate intrinsic neuronal excitability postsynaptically and extrasynaptically (Pinheiro & Mulle 2006, Contractor *et al.* 2011, Tomita & Castillo 2012, Griffith & Swanson 2015, Wyeth *et al.* 2017).

Interestingly, variants in KAR subunit genes have been associated with psychiatric disorders in human, e.g. *GRIK2* variants associate with OCD (Mattheisen *et al.* 2015) and *GRIK5* variants associate with bipolar disorder (BP) (Gratacòs *et al.* 2009). *GRIK2* is also a potential susceptibility gene for BP (Shaltiel *et al.* 2008). Moreover, changes in anxiety-like behaviour have been observed in *Grik1* and *Grik4* subunit knock-out (KO) mice. GRIK1 absence or inhibition locally in BLA increased anxiety (Wu *et al.* 2007), while *Grik4* ablation reduced anxiety and promoted an antidepressant-like behaviour (Catches *et al.* 2012). Furthermore, *Grik2* is important for fear memory in mice, i.e. *Grik2* KO mice

showed reduced freezing at 1, 3, 7 and 14 days after training in fear conditioning paradigms to both cue and context (i.e. environment) compared to wild-type (WT) mice (Ko *et al.* 2005).

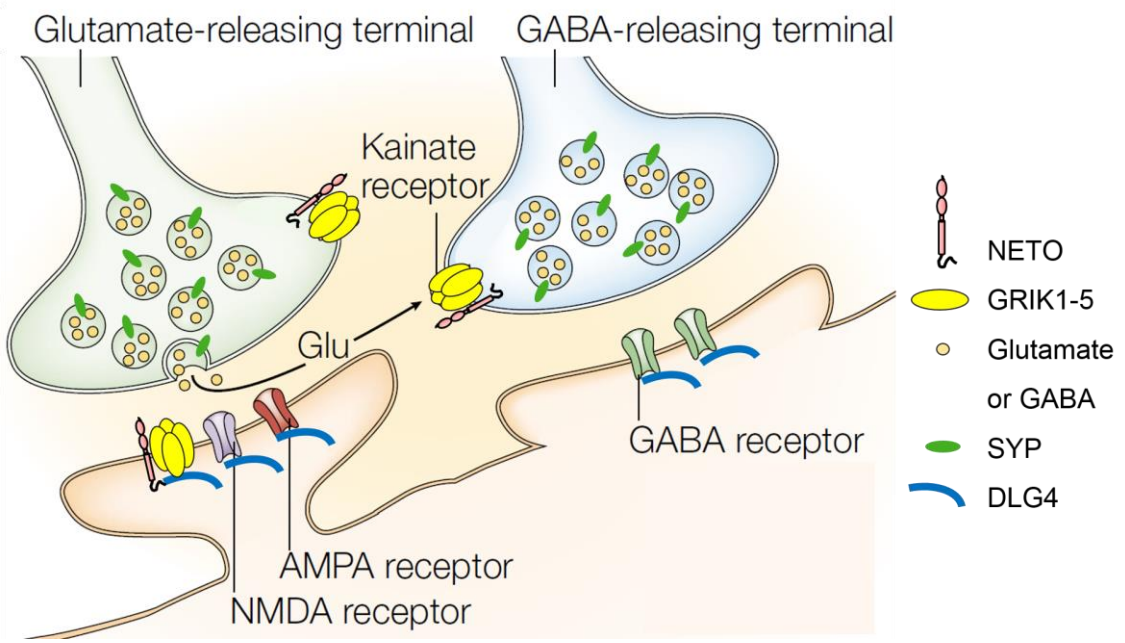


**Figure 3. Kainate receptors at synaptic sites.** Illustration of an excitatory (glutamatergic) and an inhibitory (GABAergic) synapse where KARs are present at either pre- or postsynaptic sites or at both sites. Synaptophysin (SYP) and DLG4 are well-known markers for pre- and postsynaptic regions, respectively. Synapses modified from Lerma J. (2003) and NETO protein modified from Copits & Swanson (2012). AMPA: α-amino-3-hydroxy-5-methyl-4-isoxazolepropionic acid, NMDA: N-methyl-D-aspartate, GABA: γ-aminobutyric acid.

In conclusion, KARs are important modulators of neuronal activity and disruption in KAR-mediated modulation could be sufficient to give rise to a variety of neuropsychiatric symptoms.

### 1.3. NETO proteins

Neuropilin and tolloid-like proteins NETO1 and NETO2 are homologous transmembrane CUB (complement C1r/C1s, Uegf and Bmp1) domain-containing proteins (Griffith & Swanson 2015) (Figure 4) expressed widely in the brain, including in the fear-related brain regions (i.e. amygdala, mPFC and vHPC) (Marie Mennesson, manuscript in

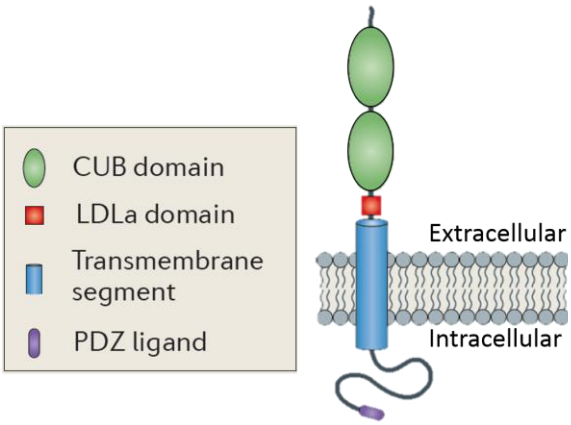


**Figure 4. Structure of NETO1 and NETO2.** NETOs bind to KARs through their CUB domains (Tang *et al.* 2011). Figure adapted from Copits & Swanson (2012). **CUB:** Complement C1r/C1s, Uegf and Bmp1; **LDLa:** low-density lipoprotein class A; **PDZ ligand:** binds PDZ domain-containing proteins (PDZ from postsynaptic density protein-95, drosophila disc large tumour suppressor, and zonula occludens-1 protein).

preparation; Ng *et al.* 2009). Moreover, a recent study has shown that they are both expressed in different interneuron populations in hippocampus (i.e. somatostatin [SOM]-, cholecystokinin/cannabinoid receptor 1 [CCK/CB1]- and parvalbumin [PV]-expressing neurons) together with *Grik1*, *Grik2* and *Grik5* KAR subunits (Wyeth *et al.* 2017). NETO proteins were recently discovered as auxiliary subunits of KARs (Zhang *et al.* 2009). They associate with KARs *in vivo* as demonstrated by co-immunoprecipitation experiments (Zhang *et al.* 2009, Straub *et al.* 2011, Tang *et al.* 2011, Tang *et al.* 2012). Additionally, NETO1 also associates with N-methyl-D-aspartate receptors (NMDARs) (Ng *et al.* 2009, Cousins *et al.* 2013), while NETO2 associates with the neuron-specific $K^+$-$Cl^-$ cotransporter KCC2 (Ivakine *et al.* 2013). In relation to NMDAR, *Neto1* KO mice were found to have impaired hippocampal-dependent spatial learning, as concluded from Morris water maze task and pharmacological rescue experiments (Ng *et al.* 2009). *Neto2* KO mice are more susceptible to seizures in correlation with decreased GABAergic inhibition and reduced KCC2 surface levels (Mahadevan *et al.* 2015).

NETO proteins modulate KAR biophysical properties in a receptor subunit- and NETO isoform-dependent manner (Fisher & Mott 2012, Fisher J.L. 2015, Griffith & Swanson 2015). For example, they modulate KAR deactivation and desensitisation rates, modal gating, agonist sensitivity, and neuronal localisation (Zhang *et al.* 2009, Copits *et al.* 2011, Straub *et al.* 2011, Tang *et al.* 2011, Tang *et al.* 2012, Fisher & Mott 2013, Wyeth *et al.* 2014, Palacios-Filardo *et al.* 2014, Zhang *et al.* 2014, Sheng *et al.* 2015, Fisher J.L. 2015, Griffith & Swanson 2015, Lomash *et al.* 2017). Interestingly, NETO1 has been shown to have a role in development, specifically regulating the hippocampal

glutamatergic connectivity through regulation of axonal KARs (Orav *et al.* 2017). Also, NETO proteins seem to regulate KAR subunit synaptic targeting (Copits *et al.* 2011, Pahl *et al.* 2014, Palacios-Filardo *et al.* 2014, Wyeth *et al.* 2014, Sheng *et al.* 2015, Evans *et al.* 2017, Lomash *et al.* 2017). Recent studies have shown that postsynaptic abundance of GRIK2 subunit is regulated by NETO2 in the cerebellum (Tang *et al.* 2012) and by NETO1 in the hippocampus (Tang *et al.* 2011), while the overall GRIK2, and additionally GRIK5, protein level in these two brain regions is unaffected by NETO2 and NETO1 absence, respectively (Tang *et al.* 2011, Tang *et al.* 2012).

To conclude, in line with KAR involvement in anxiety- and fear-related phenotypes and as an important modulator of KAR functions, NETOs may also regulate anxiety and fear in mammals.

### 1.4. Motivation, hypothesis and aims

There are currently no publications on anxiety- and fear-related behaviours in *Neto* KO mice. Previous behavioural experiments carried out in the Hovatta group revealed higher fear expression and impaired fear extinction using the cued fear conditioning paradigm (Figure 2) in *Neto2* KO mice compared to their WT littermates (Mennesson et al, manuscript in preparation). In this same paradigm, *Neto1* KO mice did not express any behavioural differences from the WT mice. Consequently, this motivated us to investigate the molecular basis of the *Neto2* KO fear phenotype.

We hypothesised that absence of NETO2 reduces KAR subunit protein levels at the synapses of fear-related brain regions, i.e. vHPC, amygdala and mPFC (Figure 1). We specifically investigated GRIK2/3 and GRIK5 levels, as antibodies are available only for these subunits, in the subcellular synaptosomal fraction (containing both pre- and postsynaptic regions) in *Neto2* WT versus KO mice.

The aims of this thesis project were the following:

- To optimise the synaptosomal enrichment method using differential centrifugation
- To validate synaptic protein enrichment in synaptosomal fractions using specific markers

- To investigate if *Neto2* WT and KO mice differ in synaptosomal KAR subunit abundance of fear-related brain regions and cerebellum

## 2. Materials and methods

### 2.1. Animals and brain dissection

*Neto2* WT and KO mice used for this study were of mixed background of C57Bl/6J and C57Bl/6N strains and were a gift from prof. R.R. McInnes (McGill University, Montréal, QC, Canada). Animals were maintained by the Laboratory Animal Centre (LAC) of the University of Helsinki. They were group housed in individually ventilated cages (IVCs) in a 12 h light/dark cycle (6am-6pm light ON) with food and water present *ad libitum*. Animal use for tissue collection was approved by LAC internal licence KEK16-011 and carried out in accordance with directive 2010/63/EU of the European Parliament and of the Council, and with the Finnish Act on the Protection of Animals Used for Science or Educational Purposes (497/2013).

Brain tissue samples were obtained from 12 weeks old male and female *Neto2* WT (*n* = 29) and KO (*n* = 21) mice. Most of the dissections were performed by Marie Mennesson (PhD student, co-supervisor of this thesis) during 2016-2017 but I dissected the last group of mice in August 2017. Rapidly after dislocation, mouse brain was extracted, rinsed with ice-cold phosphate-buffered saline (PBS) (137 mM NaCl , 2.7 mM KCl, 8.1 mM $Na_2HPO_4\,2H_2O$, 1.76 mM $KH_2PO_4$, pH = 7.4) and placed in a brain block. Micropunch dissection method was used to obtain mPFC and amygdala. Briefly, brain slices were obtained by insertion of stainless steel blades inside of the brain block (Figure 5A and 5B, zero blade inserted at the anterior part of the hypothalamus or Hyp). Dissection of mPFC was done from the two brain slices between blades +3 and +1 (Figure 5C, prelimbic/infralimbic area and cingulate cortex) and amygdala from one brain slice between blades 0 and -2 (Figure 5D). Brain slices were briefly frozen using dry ice and punched with a 16 gauge needle (Figure 5C and 5D). Punches were carefully transferred

into safe-lock tubes and immediately snap frozen in liquid nitrogen. After that, vHPC and cerebellum were extracted from the remaining part of the brain and snap frozen the same way. Tissue samples were stored at -80°C.

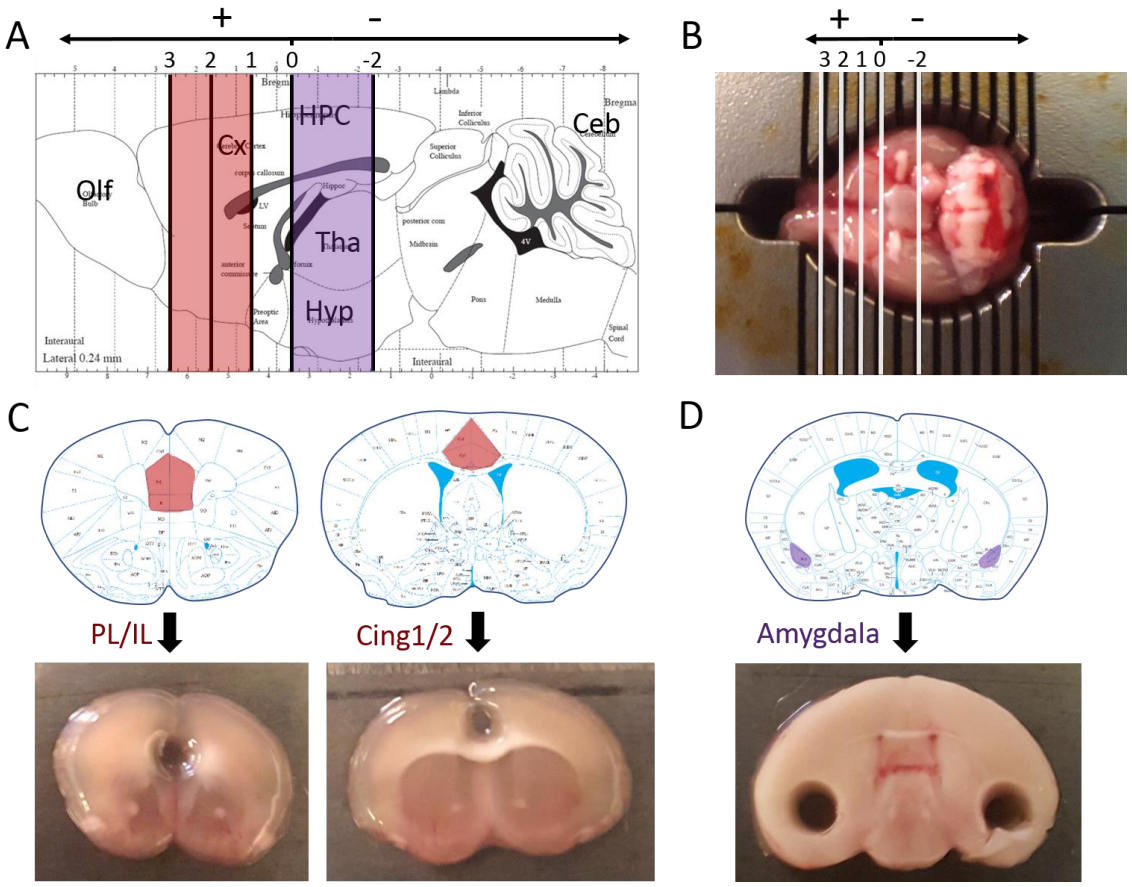


**Figure 5. Dissection of the mPFC and amygdala using the micropunch method. A.** Mouse brain atlas sagittal section and **B**. brain block showing the locations of inserted blades to obtain the brain slices used for micropunch dissection. Medial prefrontal cortex (mPFC) was obtained from two slices between +3 and +1 (marked in red in **A**) and amygdala from one slice between 0 and -2 (marked in purple in **A**). **C.** mPFC subregions (i.e. prelimbic and infralimbic area and cingulate cortex; marked in red on a mouse brain atlas coronal section) were obtained from two punches in 1 mm thick brain slices (i.e. one punch per slice). **D.** Amygdala nuclei (marked in purple on a mouse brain atlas coronal section) were obtained from two punches in a 2 mm thick brain slice (i.e. one punch per hemisphere). This figure is modified from Marie Mennesson's dissection protocol (unpublished). Mouse brain atlas figures are adapted from Franklin & Paxinos (2007). Olf: olfactory bulb, Cx: cerebral cortex, HPC: hippocampus, Ceb: cerebellum, Tha: thalamus, Hyp: hypothalamus, PL: prelimbic area, IL: infralimbic area, Cing1/2: cingulate cortex area 1 and 2.

## 2.2. Subcellular fractionation

While being blind to genotype, frozen brain tissues were transferred into Precellys24 tubes together with 500 µL ice-cold buffer A (0.32 M sucrose, 4 mM HEPES and protease cocktail, pH = 7.4) and homogenised using Precellys24 tissue homogeniser (Bertin Instruments, Montigny-le-Bretonneux, France) at a speed of 5,000 RPM for 30 s. To preserve proteins from degradation, phosphatase inhibitors were added to the homogenised samples (1:100, Sigma-Aldrich, St. Louis, MO, USA) prior to a 30 min incubation on ice. From the resulting homogenate (H), 50 µL were collected as H fraction sample (stored at -80°C) and the rest underwent differential centrifugation as previously described to obtain enriched synaptosome fraction (Maccarrone & Filiou, 2015) (Figure 6). Ultracentrifugation steps were carried out in the Center for Virus and

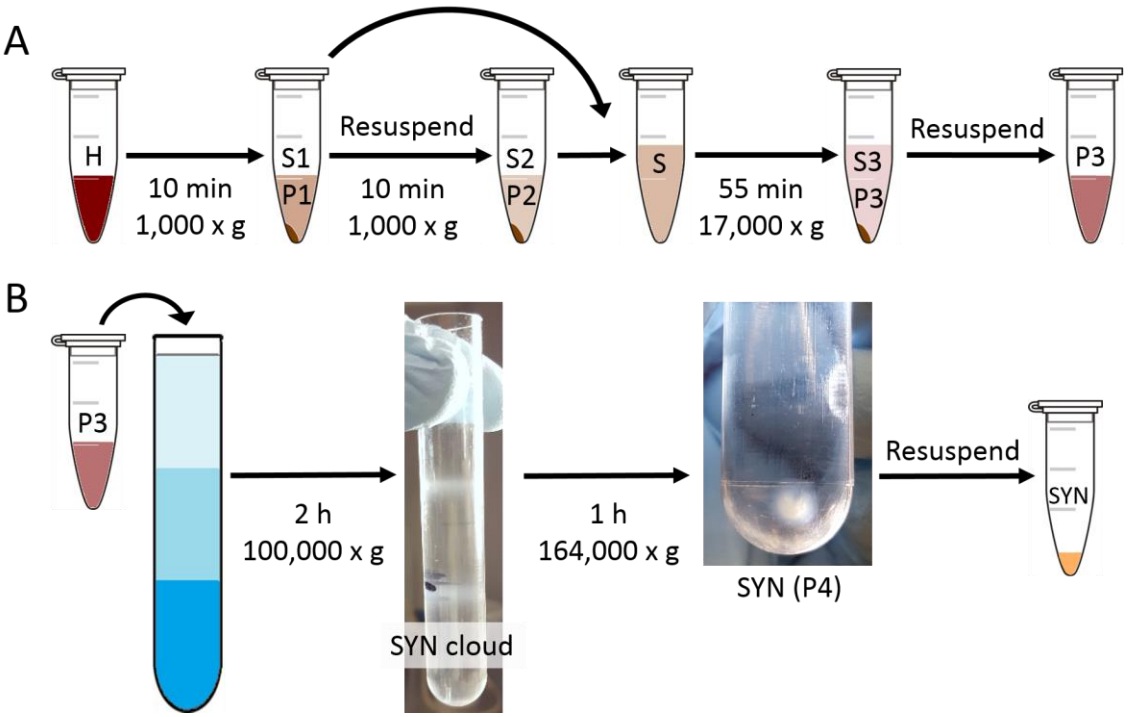


**Figure 6. Differential centrifugation and ultracentrifugation for subcellular fractionation. A.** Centrifugation of brain tissue homogenate (H) was followed by retainment of supernatant S1 and re-suspension of pellet P1 with buffer A, which underwent the same centrifugation step once more. Obtained S2 and S1 were combined (S) and P2 was discarded (containing nuclei and cell debris). After S centrifugation step, S3 was removed and P3 (containing membrane fraction with intact synaptosomes) was re-suspended in 0.32 M sucrose in 6 mM Tris (pH = 8.0). **B.** Re-suspended P3 was laid on top of a discontinuous sucrose density gradient (darkest to lightest blue represent 1.2 M, 0.8 M and 0.32 M sucrose in 6 mM Tris, pH = 8.0) and ultracentrifuged. The resulting synaptosomal (SYN)

cloud present at the 0.8 M/1.2 M interphase was adjusted to 5 mL with Milli-Q® (MQ) water for the next ultracentrifugation step. Obtained P4 was re-suspended in MQ water, representing the final enriched SYN fraction used for western blot. All centrifugations were run at +4°C. Schematic Eppendorf tube modified from Meow (2012) and schematic test tube modified from Pray_For_Eliza (2011).

Macromolecular Complex Production (IVCR, Viikinkaari 9, University of Helsinki, Helsinki, Finland), currently called Biomolecular Complex Purification (Biocomplex). Concerning mPFC and amygdala, punches from 2 to 5 animals of the same sex and genotype were pooled to ensure adequate protein concentration of the samples for western blot (Table 1). Cerebellum and vHPC samples were not pooled for synaptosomal (SYN) western blots (Table 1) or for the SYN protein enrichment western blots (*n* = 3 WT cerebella / blot, see Figure 9).

**Table 1. Tissue pooling for SYN fraction triple replicate western blots (Figure 10-13)**

| Brain region | Pooling | Sex of WTs | Sex of KOs | WTs / blot | KOs / blot |
|---|---|---|---|---|---|
| Ceb | No | Male | Male | *n* = 7 | *n* = 7 |
| vHPC | No | Male | Male | *n* = 7 | *n* = 7 |
| Amg | 3-5 mice / pool | 4 males, 3 females | 4 males, 1 female | *n* = 7* | *n* = 5 |
| mPFC | 2-5 mice / pool | 2-3 males, 2 females | 3 males, 1 female | *n* = 4-5** | *n* = 4 |

Ceb: cerebellum, vHPC: ventral hippocampus, Amg: amygdala, mPFC: medial prefrontal cortex. *Two WT samples (one male, one female) in the first round were removed from analysis due to a technical issue. **One male WT sample had a volume that was enough only for one round. It was used in the third round.

### 2.3. Protein concentration measurement using Coomassie Brilliant Blue staining

Protein concentration of each sample was estimated by comparing them to a calibrator sample of known protein concentration (H calibrator: 24.63 µg/µL or SYN calibrator: 5.89 µg/µL) using a Coomassie Brilliant Blue staining (De St. Groth *et al.* 1963). To achieve proper homogenisation, loading dye containing a reducing agent (LD) (Table 2) was added to each sample (1:3-1:4 final concentration). Samples were then incubated 5 min at 85°C and 1-2 µL of each was suspended again into 5 µL of LD. After a 2 min

incubation at 85°C, the calibrator (5 or 10 µg into 5 µL LD) and samples were loaded into a 4-20% acrylamide® gel (Bio-Rad, Hercules, CA, USA). The gel was run at 120 V for 45-60 min in Tris/Glycine/SDS (TGS) running buffer (Table 2) and incubated with Coomassie staining solution (Table 2) at 37°C for 30 min. The gel was then washed 6 x 15 min in Coomassie wash buffer (Table 2) and left overnight in the same buffer at +4°C. The next day, gels were scanned and densitometry of the strongest lane of bands was determined using ImageJ 1.50i software (Figure 7). We finally calculated the concentration of our samples based on the calibrator sample's protein concentration and band intensity.

**Table 2. Reagents used for Coomassie staining and for western blot**

| | |
|---|---|
| Loading dye (LD) | 4x Laemmli sample buffer (Bio-Rad, Hercules, CA, USA) with 0.1 M DTT (Thermo Fisher Scientific, Waltham, MA, USA). |
| Tris/Glycine/SDS (TGS) running buffer | 0.025 M Trizma® base (Sigma-Aldrich, St. Louis, MO, USA), 0.192 M glycine (Sigma-Aldrich, St. Louis, MO, USA) and 0.1% SDS (Bio-Rad, Hercules, CA, USA), pH = 8.3. |
| Coomassie staining solution | 0.1 % Coomassie Brilliant Blue dye in 10% acetic acid and 30-50% ethanol |
| Coomassie wash buffer | 10% acetic acid and 30% ethanol |
| Ponceau S Acid Red staining | 0.1% Ponceau S in 5% acetic acid |
| Stripping buffer | 62.5 mM Tris (pH = 7.5) with 2% SDS (Bio-Rad, Hercules, CA, USA) and 25 mM DTT (Thermo Fisher Scientific, Waltham, MA, USA) |

DTT: dithiothreitol, SDS: sodium dodecyl sulfate

### 2.4. Western blot

To avoid degradation of the proteins caused by repeated boiling, samples (already containing 1:3-1:4 LD from the Coomassie measurement) were instead incubated at room temperature for 10-30 min. Based on the calculations from Coomassie staining, appropriate volumes of each sample was suspended into 5 µL LD. Samples were then incubated 2 min at 85°C, quickly loaded into wells of 4-20% polyacrylamide® gels (Bio-Rad, Hercules, CA, USA) and run at 120 V for 45-60 min in TGS buffer. Proteins were

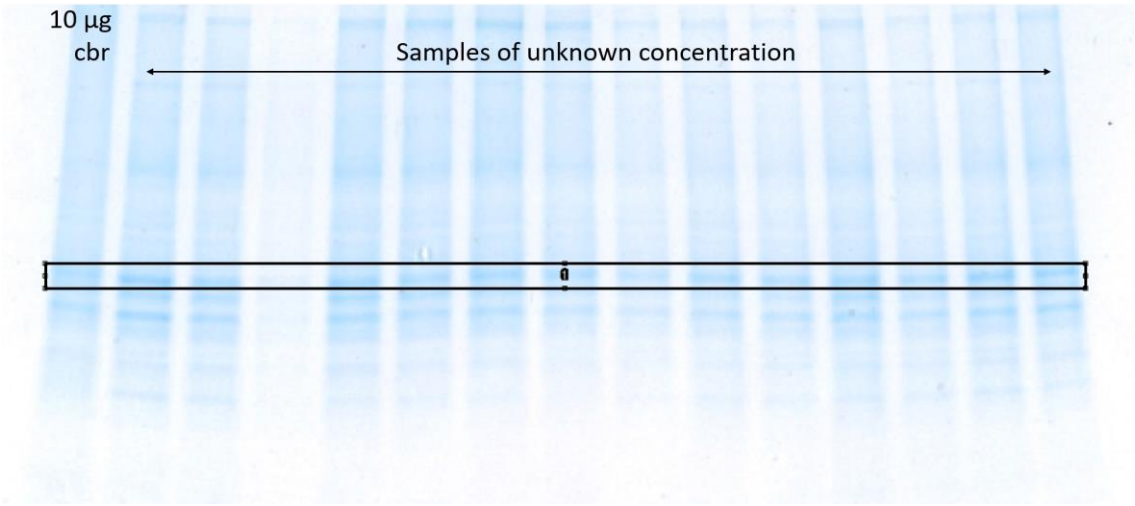


**Figure 7. Example Coomassie Brilliant Blue staining for protein concentration measurement.** Acrylamide® gel with a 10 µg calibrator sample (cbr) and 14 ventral hippocampal SYN fraction samples of unknown protein concentrations stained with Coomasssie staining. Densitometry analysis was done on the boxed lane of bands.

transferred into nitrocellulose membranes (Bio-Rad, Hercules, CA, USA) under semi-dry conditions using the manufacturer's pre-programmed protocol of 7 minutes at 1.3-2.5 A up to 25 V for proteins of molecular weights ranging 5-150 kDa (Trans-Blot® Turbo™ Transfer System, Bio-Rad, Hercules, CA, USA). Ponceau S Acid Red staining (Table 2) was used to detect successful transfer of protein (Figure 8). Membranes were then washed 3 x 5 min with Tris-buffered saline (TBS) (25 mM Tris, 15.4 mM NaCl, pH = 7.4), followed by 3 x 5 min washes with TBS-T (TBS with 0.1% TWEEN® 20, Sigma-Aldrich, St. Louis, MO, USA). Membranes were then incubated for 1 h in saturation solution depending on the primary antibody (Table 3) followed by overnight or over the weekend incubation at +4°C with primary antibody (rotation). The next day, membranes were washed 3 x 5 min with TBS-T and then incubated with secondary antibodies conjugated to horse radish peroxide (HRP) in the same saturation solution used for the primary antibody (Table 3). After 1.5 h incubation at room temperature, membranes were washed 3 x 5 min with TBS-T and then 2 x 5 min with TBS. To read bands of our proteins of interest, 1 mL of each reagent from Pierce™ ECL Western Blotting Substrate (Thermo Fisher Scientific, Waltham, MA, USA) were mixed and distributed equally on the membrane. Chemiluminescence signal was read using either G:BOX from Syngene or BioSpectrum Imaging System from UVP. Membranes were washed with 2 x 5 min TBS and stripped when necessary (e.g. if the primary antibody used next was from the same species).

Stripping was done by membrane incubation in stripping buffer (Table 2) during 30 min at 65-70°C. After this, membranes were washed 2 x 5 min with TBS and prepared for the next primary antibody staining.

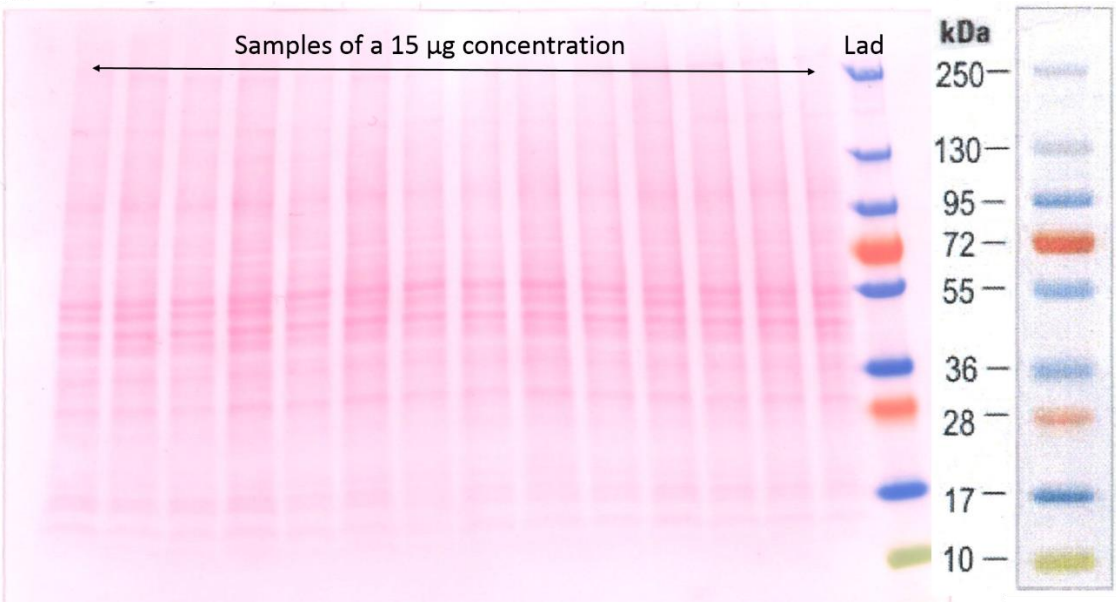


**Figure 8. Example of Ponceau S Acid Red staining to validate successful protein transfer.** Nitrocellulose membrane with 14 ventral hippocampal SYN fraction samples stained with Ponceau S. Schematic ladder adapted from manufacturer's product information booklet (Thermo Fisher Scientific, Waltham, MA, USA). Lad: Prestained Protein Ladder.

Concerning blot image analysis, background noise was reduced using Corel PHOTO-PAINT 2017 software and densitometry of blot bands were analysed using ImageJ 1.50i software. Optical densitometry results of proteins of interest were normalised using a ubiquitous protein densitometry result (actin, beta [ACTB]).

### 2.5. Statistical analyses

IBM SPSS Statistics24 software was used to run statistical analysis on the data. Data was assumed to be normally distributed. Hence, independent Student's t-test was used to compare groups (i.e. subcellular fractions or genotypes) with a 95% confidence interval.

**Table 3. Antibodies and saturation solutions used in western blot**

| Antigen | Company | Catalogue no. | Host animal | AB type | Concentration | Saturation solution |
|---|---|---|---|---|---|---|
| ACTB | Sigma-Aldrich, St. Louis, MO, USA | A1978 | Mouse | Primary | 1:2000 | 10 % milk in TBS-T |
| GRIK2/3 | Merck Millipore, Darmstadt, Germany | 04-921 | Rabbit | Primary | 1:1000 | 10 % milk in TBS-T |
| GRIK5 | Merck Millipore, Darmstadt, Germany | 06-315 | Rabbit | Primary | 1:1000 | 10 % milk in TBS-T |
| NETO2 | Gift from prof. R.R. McInnes, McGill University, Montréal, QC, Canada | | Rabbit | Primary | 1:1000 | 10 % milk in TBS-T |
| DLG4 | Santa-Cruz Biotechnology, Dallas, TX, USA | sc-32290 | Mouse | Primary | 1:1000 | 3% BSA in TBS-T |
| SYP | Sigma-Aldrich, St. Louis, MO, USA | S5768 | Mouse | Primary | 1:300 | 5% BSA in TBS-T |
| Rabbit AB | Jackson ImmunoResearch, West Grove, PA, USA | 111-035-144 | Goat | Secondary | 1:5000 | Same as primary AB |
| Mouse AB | Jackson ImmunoResearch, West Grove, PA, USA | 115-035-146 | Goat | Secondary | 1:5000 | Same as primary AB |

AB: antibody, TBS-T: Tris-buffered saline with 0.1% TWEEN® 20, BSA: bovine serum albumin

# 3. Results

## 3.1. Successful synaptosomal protein enrichment

To validate the synaptosomal enrichment method, we first compared the protein level of obtained H and SYN fractions from WT cerebellum samples. The reason why we used cerebellum is because of its high *Neto2* expression and NETO2 protein level (Michishita *et al.* 2004, Straub *et al.* 2011, Tang *et al.* 2012), and thus we justified it as a positive control. Ubiquitously expressed ACTB protein served as an inter-sample control for equal total protein loading, which successfully showed no statistically significant difference between fractions in either blot (Reference blot: $P$ = .07 and KAR blot: $P$ = .39) (Figure 9A-D). Pre- and postsynaptic markers (i.e. SYP and DLG4, respectively, Figure 3), and our proteins of interest (i.e. NETO2, GRIK2/3 and GRIK5) were used to confirm the actual enrichment. SYN fraction contains both pre- and postsynaptic compartments. Hence, a higher concentration of SYP and DLG4 in SYN fraction compared to H confirmed

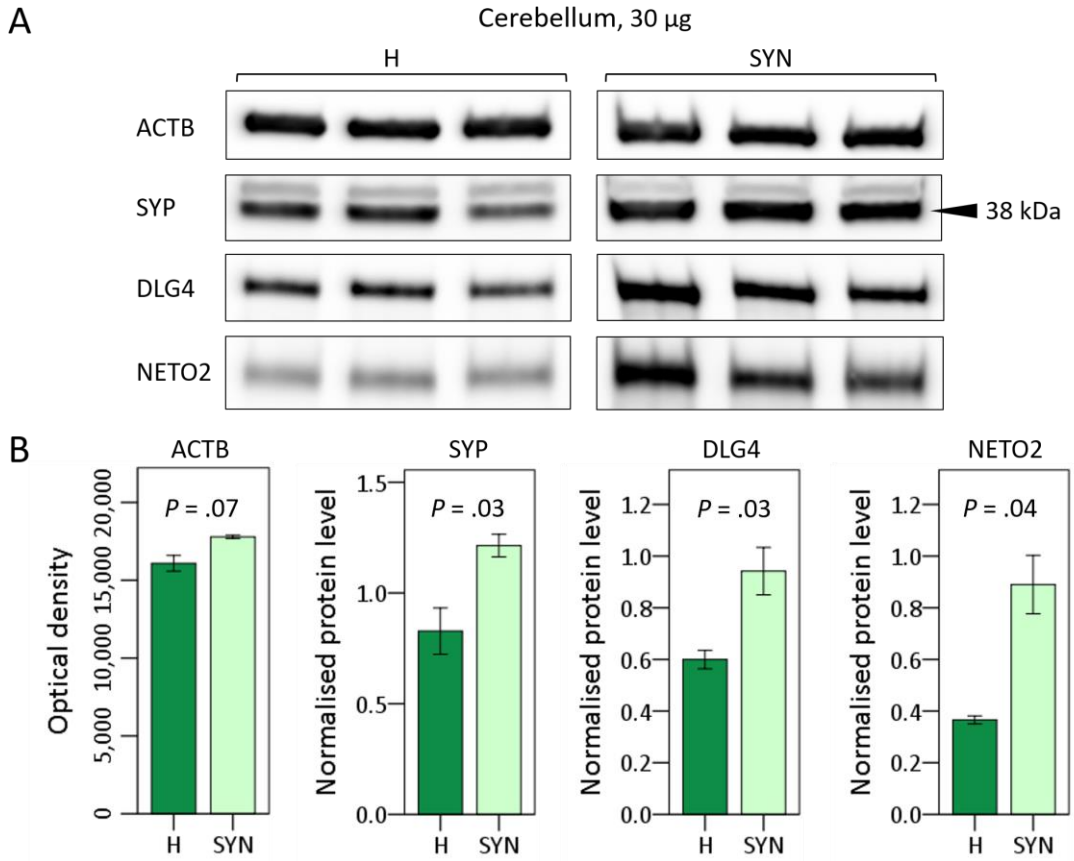

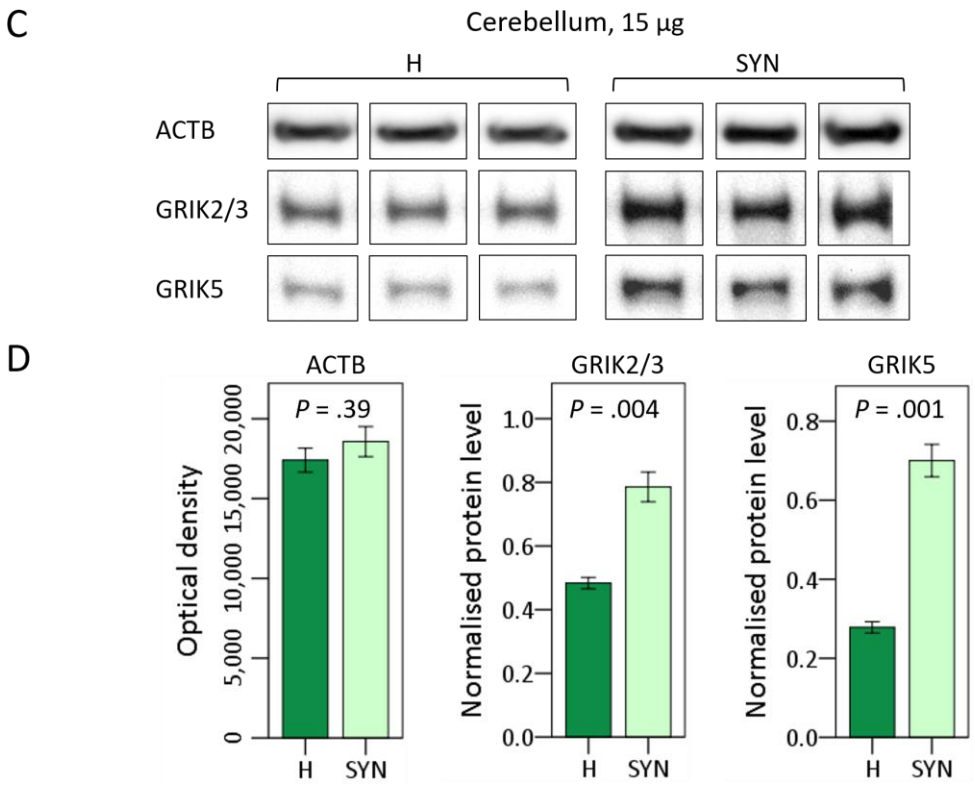


**Figure 9. Successful enrichment of synaptosomal proteins. A-B.** Reference blots. **C-D.** KAR blots. Full blots in Appendix 1. **A & C:** Western blots of H and SYN fractions from WT cerebella. **B & D:.** Protein level of (**B**) DLG4, SYP, NETO2, (**D**) GRIK2/3 and GRIK5 normalised using ubiquitously expressed ACTB. Error bars represent +/- 1 standard error of the mean. *n* = 3 males / blot.

a successful SYN fractionation (*P* = .03 for both proteins) (Figure 9A and 9B). Our proteins of interest NETO2, GRIK2/3 and GRIK5 are also known to be concentrated at synapses. Therefore, as expected, they also showed enrichment in SYN fraction compared to the H fraction (*P* = .04, .004 and .001, respectively) (Figure 9A-D).

### 3.2. KAR subunit abundance in cerebellum and fear-related brain regions is not affected by NETO2 absence

We next tested our main question, i.e. the effect of *Neto2* ablation on KAR abundance at synapses in fear-related brain regions. Additionally, we were interested in the cerebellum, since *Neto2* KO mice show a 40% reduction of GRIK2 subunit containing KARs at the postsynaptic density (PSD) in this brain region (Tang *et al.* 2012). As both

*Neto2* expression and NETO2 protein level is the highest in cerebellum compared to other brain regions (Michishita *et al.* 2004, Straub *et al.* 2011, Tang *et al.* 2012), we wanted to test if its ablation also affects KAR subunits in SYN fractions (i.e. contain both pre- and postsynaptic fractions). We confirmed NETO2 absence from the KO mice cerebella ($P$ = .000003) (Figure 10). Nevertheless, there was no statistically significant difference in GRIK2/3 ($P$ = .41) or GRIK5 ($P$ = .77) abundance between genotypes in the cerebellum (Figure 10B). Thus it seems that the GRIK2 reduction observed by Tang *et al*. (2012) is specific to PSD.

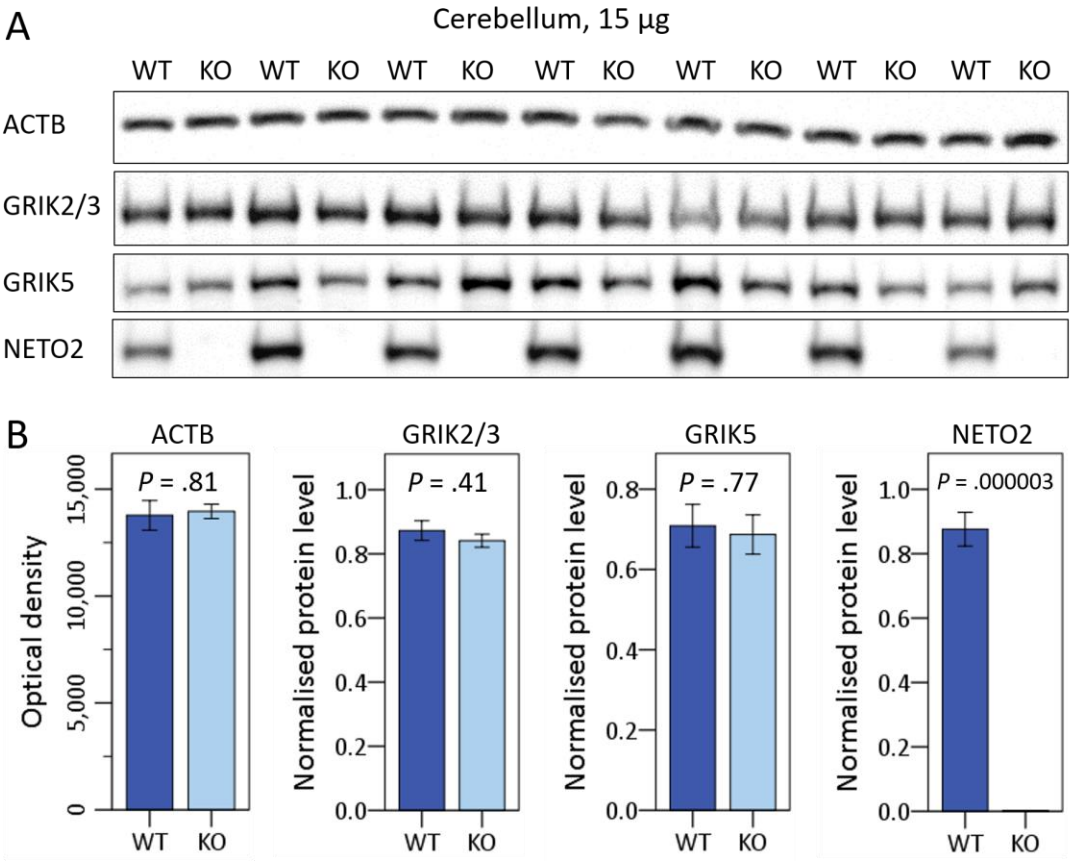


**Figure 10. Synaptic KAR subunit abundance in cerebellum is unaffected by NETO2 absence.** **A**. Representative blots of cerebellar SYN fractions from *Neto2* WT and KO mice. Full blots in Appendix 2. **B**. Protein level of GRIK2/3, GRIK5 and NETO2 normalised using ubiquitously expressed ACTB. Each sample value was obtained from three blot replicates (WT $n$ = 7, KO $n$ = 7). Error bars represent +/- 1 standard error of the mean.

The neural circuitry underlying learning in the fear conditioning paradigm includes an interplay between the vHPC, amygdala and mPFC, as reviewed by Maren and Holmes (2016). Consequently, we investigated these brain regions, starting with the vHPC,

which is important for the representation of the context of acquired fear memory (Maren & Holmes 2016). We confirmed NETO2 absence from the KO mice vHPC (*P* = .0004) (Figure 11). As observed in the cerebellum, there was no statistically significant difference in GRIK2/3 (*P* = .44) or GRIK5 (*P* = .46) abundance between genotypes in the vHPC (Figure 11B).

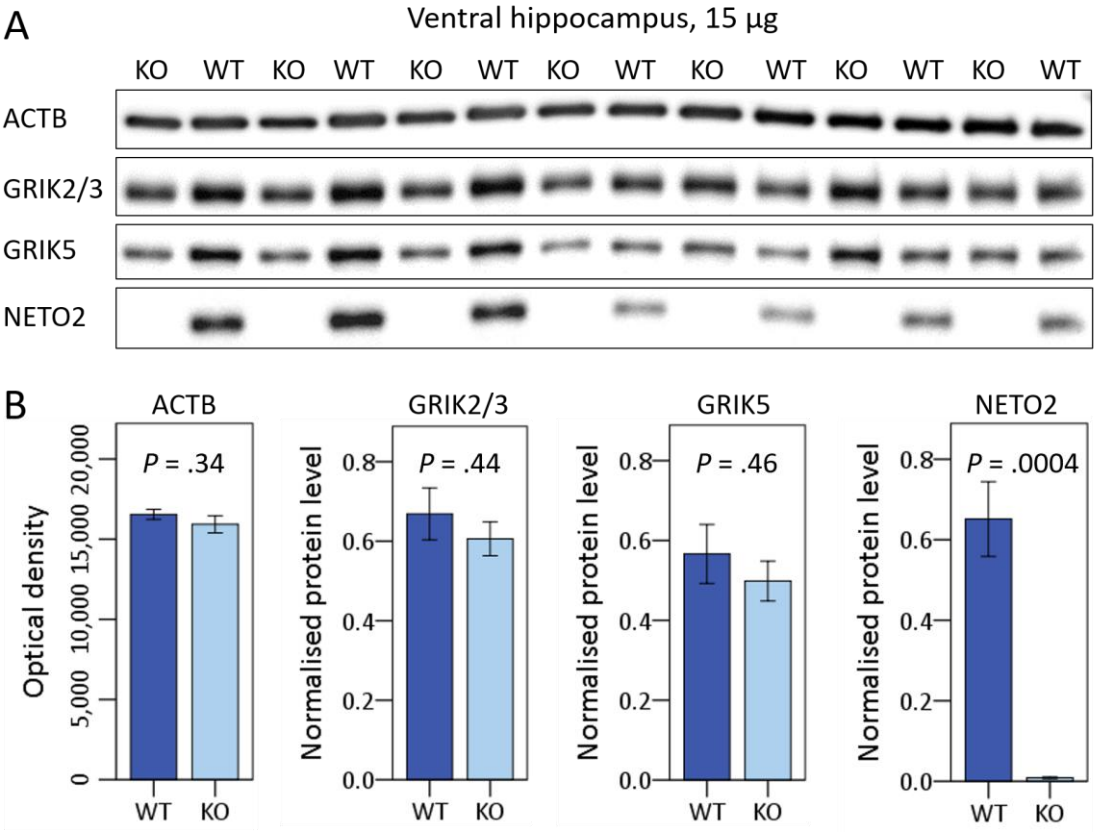


**Figure 11. Synaptic KAR subunit abundance in vHPC is unaffected by NETO2 absence.** **A**. Representative blots of ventral hippocampal SYN fractions from *Neto2* WT and KO mice. Full blots in Appendix 3. **B**. Protein level of GRIK2/3, GRIK5 and NETO2 normalised using ubiquitously expressed ACTB. Each sample value was obtained from three blot replicates (WT *n* = 7, KO *n* = 7). Error bars represent +/- 1 standard error of the mean.

Amygdala is crucial for fear conditioning, as it is the center of emotional learning (Maren & Holmes 2016). As for the other brain regions we investigated, we confirmed NETO2 absence also from KO mice amygdalae (*P* = .008) (Figure 12). Contrary to our hypothesis, we also did not observe statistically significant difference in GRIK2/3 (*P* = .40) or GRIK5 (*P* = .81) abundance between genotypes in the amygdala (Figure 12B). However, due to pooling, the final number of samples was lower for the amygdala compared to the other

brain regions. In addition, we also observed a high variation between samples (Figure 12B). Therefore, our statistical power was likely insufficient to detect possible small changes in GRIK2/3 and GRIK5 abundance between WT and KO mice (Figure 12B).

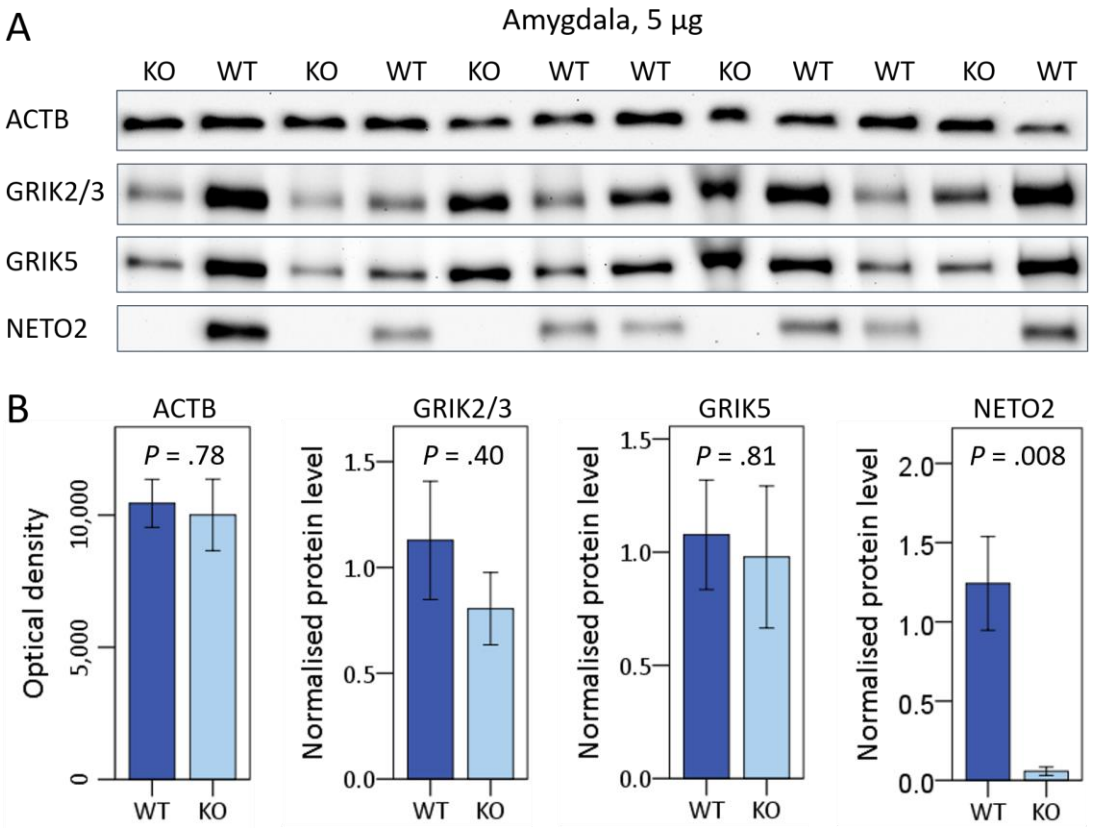


**Figure 12. Synaptic KAR subunit abundance in amygdala is unaffected by NETO2 absence.** **A**. Representative blots of amygdalar SYN fractions from *Neto2* WT and KO mice. Full blots in Appendix 4. **B**. Protein level of GRIK2/3, GRIK5 and NETO2 normalised using ubiquitously expressed ACTB. Each sample value was obtained from three blot replicates (WT *n* = 7, KO *n* = 5). Error bars represent +/- 1 standard error of the mean.

Finally, we studied the mPFC, which plays an important role in fear memory extinction and fear expression (Maren & Holmes 2016). Also in this brain region we confirmed NETO2 absence from KO mice (*P* = .008) (Figure 13). As in the other brain regions we investigated, there was no statistically significant difference in GRIK2/3 (*P* = .21) and GRIK5 (*P* = .14) abundance between genotypes in the mPFC either (Figure 13B). However, limiting factors were present, such as a small number of samples and a high variation between samples (Figure 13B). Thus, once again, our statistical power was

possibly insufficient to detect potential small differences in GRIK2/3 and GRIK5 abundance between WT and KO mice (Figure 13B).

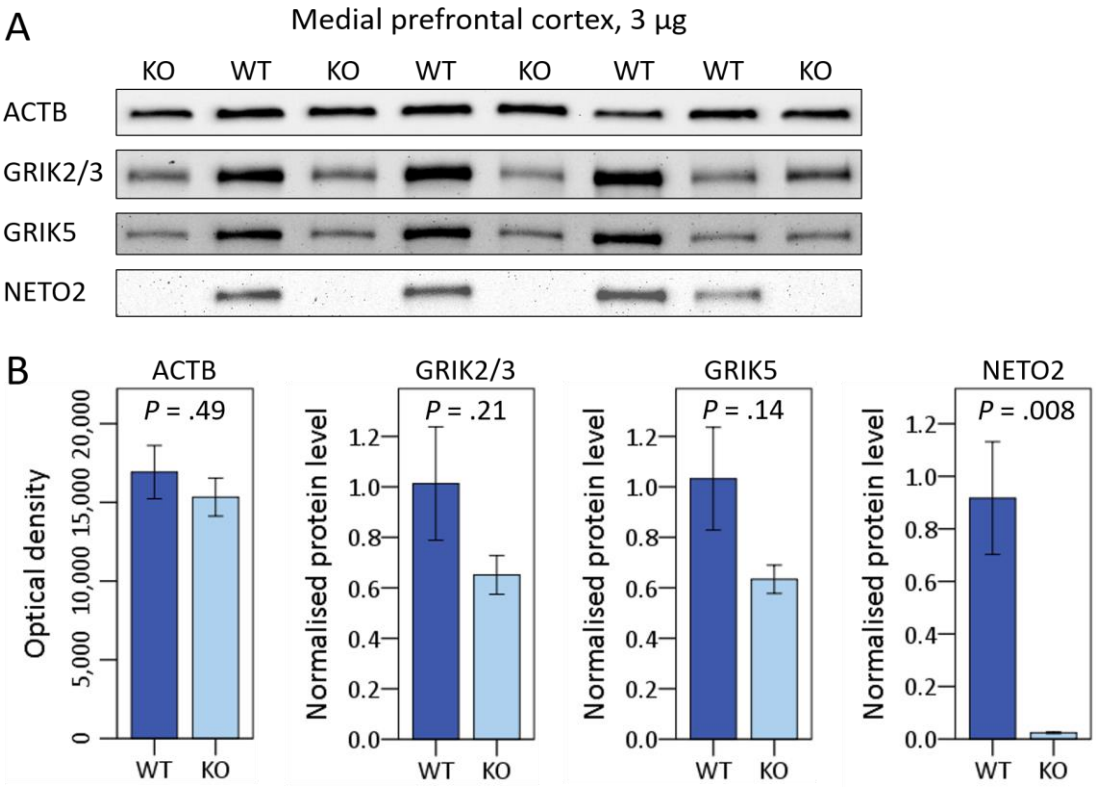


**Figure 13. Synaptic KAR subunit abundance in mPFC is unaffected by NETO2 absence.** **A**. Representative blots of mPFC SYN fractions from *Neto2* WT and KO mice. Full blots in Appendix 5. **B**. Protein level of GRIK2/3, GRIK5 and NETO2 normalised using ubiquitously expressed ACTB. Each sample value was obtained from three blot replicates (WT *n* = 4-5, KO *n* = 4). Error bars represent +/- 1 standard error of the mean.

## 4. Discussion

This study investigated the molecular basis of the higher fear expression and impaired fear extinction phenotype previously observed in *Neto2* KO mice. We hypothesised that this phenotype could be partly due to reduced KAR subunit levels at synapses of fear-related brain regions (i.e. vHPC, amygdala and mPFC) (Maren & Holmes, 2016) (Figure 1). *Neto2* is highly expressed in cerebellum (Michishita *et al.* 2004, Tang *et al.* 2012),

thus we also measured KAR subunit abundance in this brain region. Moreover, a previous study demonstrated a 40% reduction of GRIK2 subunit containing KARs at cerebellar PSD of *Neto2* KO mice (Tang *et al.* 2012).

In this study we used an enrichment method that allowed us to investigate protein abundance at pre- and postsynaptic compartments (i.e. synaptosome or SYN fraction) and we determined protein concentrations semi-quantitatively using western blot. Restricted by commercially available antibodies, we investigated GRIK2/3 and GRIK5 subunit levels in SYN fractions of *Neto2* WT and KO mice. We first confirmed synaptosome enrichment in obtained SYN fractions using well-known pre- and postsynaptic markers SYP and DLG4, which recognise presynaptic vesicles and the postsynaptic density, respectively (Figure 3).

We did not observe any statistically significant differences between genotypes for GRIK2/3 and GRIK5 levels in any of the four brain regions. These results are discussed further in the context of the literature.

### 4.1. Enrichment validation using synaptosome markers

We validated our synaptosomal enrichment method using pre- and postsynaptic markers SYP and DLG4. These two proteins play specific roles at synapses and are commonly used as markers for synaptosomal enrichment. SYP is a vesicular transmembrane protein that is present only at presynaptic compartment and DLG4 is a protein that interacts with receptors, ion channels and many other proteins at the postsynaptic compartment (Figure 3). As expected, the abundances of these markers were higher in SYN fractions compared to tissue homogenates (H), and thus confirming the enrichment.

We decided that the SYP and DLG4 markers were sufficient to validate enrichment of our SYN fractions, as our method was based on previously published studies (Filiou *et al.* 2010, Maccarrone & Filiou 2015). They validated the synaptosomal enrichment by showing the change of specific compartment markers along the process of subcellular fractionation, i.e. they compared synaptosomes to fractions obtained earlier in the

protocol (e.g. nuclear fraction [P2] and SYN-fraction-free supernatant [S3], see Figure 6) by using markers such as synaptosome-specific DLG4 and non-synaptosomal marker myelin basic protein (MBP). An additional method for confirming obtainment of synaptosomes would be to visualise subcellular components in our SYN fractions by using electron microscopy. SYN fractions contain synaptic membranes, mitochondria, synaptic vesicles, PSDs and black bodies, which are probably condensed nerve-ending particles (Gray & Whittaker, 1962).

### 4.2. NETO2 absence does not affect KAR subunit abundance in cerebellum

NETO2 is highly abundant in cerebellum (Straub *et al.* 2011) and has been previously shown to modulate and/or stabilise KAR subunit abundance in cerebellar PSD fractions (Tang *et al.* 2012). Nonetheless, we did not observe any statistically significant difference in GRIK2/3 or GRIK5 abundance between genotypes in our SYN fractions. Interestingly, Tang *et al*. (2012) demonstrated a 40% reduction in GRIK2 subunit containing KARs in *Neto2* KO cerebellar PSD fractions. Notably, they performed a PSD fraction enrichment method while we obtained synaptosomes, and thus these studies are not technically comparable. Also, absence of NETO2 could change GRIK2 abundance in opposite directions at pre- and postsynaptic compartments, explaining the discrepancy between our results and the Tang *et al.* (2012) study. Furthermore, we used an antibody that recognises both GRIK2 and GRIK3 subunits while they used an antibody directed specifically against GRIK2. This technical difference may thus also contribute to the different observations of these studies, especially if GRIK3 abundance goes in an opposite direction (i.e. increased abundance when NETO2 is absent).

To conclude, against our expectations, *Neto2* ablation did not affect abundance of KAR subunits that show the highest expression level in cerebellum (i.e. *Grik2* and *Grik5*) (Watanabe-Iida *et al.* 2016). It is particularly interesting that GRIK2 and GRIK3 are not affected, since the protein levels of both are the highest in cerebellar PSD fraction compared to other KAR subunits (Watanabe-Iida *et al.* 2016). Whether regulation of synaptic KAR subunit abundance is achieved through regulation of KAR synaptic

targeting is not known, as it has never been clearly demonstrated. On one hand, the reduction of GRIK2 in *Neto2* KO cerebellar PSD fractions observed by Tang *et al.* (2012) suggests a role for NETO2 in synaptic targeting of KARs. On the other hand, Zhang *et al.* (2009) showed that over-expression of *Neto2* in *Xenopus laevis* oocytes was unable to enhance GRIK2 surface trafficking. Also, Palacios-Filardo *et al.* (2014) conclude that while NETO2 may promote synaptic localisation of endogenous KARs containing low-affinity subunits, they are unlikely to underlie synaptic trafficking of these receptors. Moreover, a recent study demonstrated that GRIK2/3 and GRIK5 levels were unaltered in cerebellar PSD-enriched fractions of *Neto2* KO mice (Straub *et al.* 2016). Thus, these studies concur with our observation in cerebellar synaptosomes. Interestingly, the opposite has been shown, i.e. GRIK2 regulates NETO2 abundance at cerebellar PSD (Straub *et al.* 2016) and at the surface of cerebellar granule cells (Zhang *et al.* 2009). Taken together, we did not detect an effect of NETO2 on KAR abundance in cerebellar synaptosomes, but these results also do not allow us to clearly demonstrate a nonexistent role for *Neto2* in KAR subunit synaptic targeting in cerebellum.

### 4.3. KAR subunit abundance is unaffected in fear-related brain regions of *Neto2* KO mice

The higher fear expression and impaired fear extinction in *Neto2* KO mice lead us to investigate KAR subunit abundance specifically in the fear-related brain regions (i.e. vHPC, amygdala and mPFC) (Figure 1). We did not observe statistically significant difference in GRIK2/3 or GRIK5 abundance between genotypes in any of these three brain regions. In the vHPC, these results are in agreement with a previous study, where NETO2 absence does not affect GRIK2 and GRIK5 abundance at hippocampal PSD (Tang *et al.* 2011). Also, a behavioural study from the Hovatta group demonstrated that *Neto2* ablation does not affect the context memory retained from fear conditioning, mostly regulated by the HPC (Mennesson *et al.* manuscript in preparation). In conclusion, our results correlate with theses previous studies and we show that NETO2 does not regulate GRIK2/3 or GRIK5 abundance specifically at vHPC synapses either. Instead, NETO2's role in the HPC may be mainly attributed to synaptic targeting of GRIK1, which

is a previously established role for NETO2 in this brain region (Copits *et al.* 2011, Sheng *et al.* 2015, Lomash *et al.* 2017). In the amygdala and mPFC, our results show that GRIK2/3 and GRIK5 are present at synaptosomes even when NETO2 is absent and that there is no statistically significant difference in their synaptic abundance between genotypes. However, variation was particularly large for these two brain regions (Figures 12B and 13B), and thus we may not have enough statistical power to detect changes in KAR subunit levels. Still, a potential reduction in synaptic GRIK5 level was observed for KO mice mPFCs (39% mean reduction, $P$ = .14), which may alter neurotransmission and/or neuron excitability in this brain region. In line with the importance of mPFC in fear expression and extinction memory, this could explain the phenotype observed in *Neto2* KO mice. If the potentially reduced abundance is specific to either pre- or postsynaptic membrane, it can be clarified by performing further subcellular fractionation to separate the two compartments. Also, we do not know if there are compensatory mechanisms in the absence of NETO2 e.g. by NETO1, which may moderate a reduction in KAR subunits. Thus, it would be interesting to investigate KAR subunit abundance in *Neto1/Neto2* double-KO (DKO) mice to see if this may further reduce KAR subunit abundance in mPFC. Alternatively, abundance of other KAR subunits not studied here due to the absence of available specific antibodies (i.e. GRIK1 and GRIK4) may be affected and contribute towards the fear-phenotype in *Neto2* KO mice.

In conclusion, NETO2 absence does not affect GRIK2/3 and GRIK5 abundance at synaptosomes in fear-related brain regions, but the statistical power may have been insufficient to detect changes in their abundances in amygdala and mPFC. Some studies support the idea of NETO proteins affecting KAR subunit abundance, while others do not (Zhang *et al.* 2009, Tang *et al.* 2011, Tang *et al.* 2012, Pahl *et al.* 2014, Straub *et al.* 2011, Straub *et al.* 2016). These seemingly contradictory observations may be attributed to different experimental conditions, subunits and cell types, which leaves NETOs' role in KAR synaptic targeting still unresolved (Pahl *et al* 2014, Evans *et al.* 2017). It is known, however, that NETO2 modulate KAR biophysical properties, such as desensitisation, current frequency, decay kinetics, inward rectification and agonist sensitivity (Zhang *et al.* 2009, Straub *et al.* 2011, Fisher & Mott 2012), and thus KAR function may change in *Neto2* KO mice while KAR subunit abundance remains unaffected.

### 4.4. Strengths and limitations

This is the first study that investigated KAR subunit abundance in the vHPC, amygdala and mPFC in *Neto2* KO mice. As such, it can provide practical guidance for future experiments on these brain regions. Presynaptic membranes were included in our synaptosomal fractions, which therefore include presynaptic KARs, while previous studies have investigated mostly PSD enriched fractions. Nonetheless, separating pre- and postsynaptic sites for comparison is preferred. Furthermore, although western blot is only a semi-quantitative method, it is presumably sufficient for our purposes of demonstrating protein enrichment and abundance.

However, western blot does not come without methodological challenges. A major challenge in this study was the small sizes of the amygdala and mPFC punches. Punches had to be pooled in order to obtain samples with adequate protein concentration and a limited number of animals were available (on average, 20 animals made only 5 pooled samples). This is also why we had to analyse pools of male and female mice together to achieve a higher *n*. Clearly, pooling sexes together is not ideal, but at least both sexes of the *Neto2* KO mice had shown higher fear expression and impaired fear extinction in the fear conditioning paradigm carried out previously by Marie Mennesson. Furthermore, boiling of the samples gave rise to smearing on the membranes for at least GRIK2/3 and GRIK5 blots, which may indicate affected integrity of sample proteins.

Another strength of our study is that we replicated our synaptosomal blots three times to increase the validity of the results. However, comparing blot to blot introduces within-sample variation, since many factors during western blot (e.g. protein loading, protein transfer efficiency, signal exposure, background signal, stripping efficiency etc.) can cause variations in the results. Nonetheless, we controlled for some of these potential causes of variation. For example, variation due to sample position on blot was controlled by changing the position for every sample in each blot.

Apart from these technical difficulties, the statistical analysis used needs to be interpreted with caution. The small number of samples (particularly for amygdala and mPFC) make the use of statistical analyses questionable as *t*-test should only be used

for normally distributed data. Testing for normal distribution on a small number of samples was problematic, and thus, normal distribution was assumed without proper confirmation.

### 4.5. Future directions

Further experiments are required to validate if there is indeed no change in GRIK2/3 or GRIK5 abundance at synapses in *Neto2* KO mice in the four brain regions studied here (i.e. increase sample number, separate sexes, increase subcellular specificity and avoid boiling samples before using them in SDS-PAGE). Confirming a potential GRIK5 reduction in mPFC of *Neto2* KO mice is particularly interesting, as the effect of *Neto2* ablation on behaviour could stem from this region. Alternatively, abundance of other KAR subunits not studied here (i.e. GRIK1 and GRIK4) may be affected. However, even if all KAR subunit levels may be unaffected by *Neto2* ablation, another possibility is an altered KAR function, which could give rise to changes in neurotransmission and/or neuron excitability. These biophysical properties can be examined through electrophysiological recordings in brain slices *in vitro,* offering a more controlled, cell-specific environment to differentiate pre- and postsynaptic neurons. For example, intrinsic excitability of infralimbic area (IL) in mPFC would be interesting to investigate, as it changes in opposite directions to allow for expression of conditioning memory or extinction memory (Santini *et al,* 2008, Bloodgood *et al.* 2018). A more challenging approach would be electrophysiological recordings *in vivo* while *Neto2* WT and KO mice are undergoing cued fear conditioning, as this is when the phenotype appears. Furthermore, using specific antibodies (i.e. GRIK2- and GRIK3-specific antibodies in our case) is of importance, as a possible role for NETO proteins in synaptic targeting of KARs most likely is subunit dependent. Finally, investigating synaptic location (i.e. pre- or postsynaptic) and abundance of KAR subunits in *Neto2* KO mice by immunological labelling using gold molecules and electron microscopy may be of interest to expose more anatomically precise changes underlying the fear-phenotype in *Neto2* KO mice.

### 4.6. Conclusions

We observed no statistically significant difference in GRIK2/3 and GRIK5 synapse abundance between genotypes in any of the four tested brain regions (i.e. cerebellum, vHPC, amygdala and mPFC). However, our statistical power may have been insufficient to detect genotypic differences in KAR subunit levels particularly in amygdala and mPFC. The effect of NETO2 absence on these subunit levels, including the potentially reduced GRIK5 level in mPFC, could be confirmed by increasing sample sizes and reducing inter-sample variation. Also, changes in abundance might be specific to certain cells, to either pre- or postsynaptic compartment and/or specific to a certain KAR subunit. Therefore, future experiments with higher cellular and subcellular specificity and specific anti-GRIK antibodies (when these are available) are suggested to confirm these possibilities. Electrophysiological recordings of brain slices *in vitro* can also be performed after cued fear conditioning to reveal potential changes in e.g. intrinsic excitability of neurons in mPFC to advance the understanding of the mechanism behind the *Neto2* KO fear-phenotype. Unraveling how a molecular system without NETO2 gives rise to higher fear expression and a fear extinction deficit in mice may lead to a better understanding of fear-related disorders in human. As NETOs regulate KAR actions and their cellular localisation, targeting NETO proteins could provide new and attractive therapeutics with more finely adjusted effects on neuronal activity to treat neuropsychiatric disorders.

## 5. References

Allen Institute for Brain Science (2018) Mouse Brain Atlas. Retrieved from http://mouse.brain-map.org/ (16.04.2018)

American Psychiatric Association (2016) Anxiety Disorder: DSM-5® Selections, DSM-5® Anxiety Disorders, e-book, Available at

http://web.b.ebscohost.com/ehost/ebookviewer/ebook/bmxlYmtfXzE2MTAyMTlfX0FO0?sid=b2a8cb94-6b3d-4612-b0bd-4f550fd1c8db@sessionmgr104&vid=0&format=EK&lpid=i1&rid=0 (29.5.2018)

Catches, J.S., Xu, J. & Contractor, A. (2012), Genetic ablation of the GluK4 kainate receptor subunit causes anxiolytic and antidepressant-like behavior in mice, *Behavioural Brain Research*, **228**(2), pp. 406-414. DOI 10.1016/j.bbr.2011.12.026.

Copits, B.A., Robbins, J.S., Frausto, S. & Swanson, G.T. (2011), Synaptic targeting and functional modulation of GluK1 kainate receptors by the auxiliary neuropilin and tolloid-like (NETO) proteins, *The Journal of Neuroscience*, **31**(20), pp. 7334-7340. DOI 10.1523/JNEUROSCI.0100-11.2011.

Cousins, S.L., Innocent, N. & Stephenson, F.A. (2013), Neto1 associates with the NMDA receptor/amyloid precursor protein complex, *Journal of Neurochemistry*, 126, pp. 554-564. DOI 10.1111/jnc.12280

De St. Groth, S.F., Webster, R.G. & Datyner, A. (1963), Two new staining procedures for quantitative estimation of proteins on electrophoretic strips, *Biochimica et Biophysica Acta*, 71, pp. 377-391. DOI 10.1016/0006-3002(63)91092-8.

Evans, A.J., Gurung, S., Henley, J.M, Nakamura, Y. & Wilkinson, K.A. (2017), Exciting Times: New Advances Towards Understanding the Regulation and Roles of Kainate Receptors, *Neurochemical Research*, pp. 1-13. DOI 10.1007/s11064-017-2450-2.

Filiou, M.D., Bisle, B., Reckow, S., Teplytska, L., Maccarrone, G. & Turck, C.W. (2010), Profiling of mouse synaptosome proteome and phosphoproteome by IEF, *Electrophoresis*, **31**(8), pp. 1294-1301. DOI 10.1002/elps.200900647

Fisher, J.L. & Mott, D.D. (2012), The auxiliary subunits Neto1 and Neto2 reduce voltage-dependent inhibition of recombinant kainate receptors, *The Journal of Neuroscience,* **32**(37), pp. 12928-12933. DOI10.1523/JNEUROSCI.2211-12.2012

Fisher, J.L. & Mott, D.D. (2013), Modulation of homomeric and heteromeric kainate receptors by the auxiliary subunit Neto1, *The Journal of Physiology*, **591**(19), pp. 4711-4724. DOI 10.1113/jphysiol.2013.256776.

Fisher, J.L. (2015), The auxiliary subunits Neto1 and Neto2 have distinct, subunit-dependent effects at recombinant GluK1- and GluK2-containing kainate receptors, *Neuropharmacology,* 99, pp. 471-480. DOI 10.1016/j.neuropharm.2015.08.018.

Franklin, K.B.J. & Paxinos, G. (2007), *The Mouse Brain in Stereotaxic Coordinates*, New York: Elsevier, Academic Press, ed.3

Gratacòs, M., Costas, J., de Cid, R., Bayés, M., González, J.R., Baca-García, E., de Diego, Y., Fernández-Aranda, F., Fernández-Piqueras, J., Guitart, M., Martín-Santos, R., Martorell, L., Menchón, J.M., Roca, M., Sáiz-Ruiz, J., Sanjuán, J., Torrens, M., Urretavizcaya, M., Valero, J., Vilella, E., Estivill, X. & Carracedo, A. (2009), Identification of new putative susceptibility genes for several psychiatric disorders by association analysis of regulatory and non-synonymous SNPs of 306 genes involved in neurotransmission and neurodevelopment, *American journal of medical genetics, Part B, Neuropsychiatric genetics,* **150B**(6), pp. 808-816. DOI 10.1002/ajmg.b.30902.

Griffith, T.N. & Swanson, G.T. (2015), Identification of critical functional determinants of kainate receptor modulation by auxiliary protein Neto2, *The Journal of Physiology*, **593**(22), pp. 4815-4833. DOI 10.1113/JP271103.

Gray, E.G & Whittaker, V.P. (1962) The isolation of nerve endings from brain: an electron-microscopic study of cell fragments derived by homogenization and centrifugation, *Journal of Anatomny*, **96**(1), pp. 79-88.

Isaac, J.T.R., Mellor, J., Hurtado, D. & Roche, K.W. (2004), Kainate receptor trafficking: physiological roles and molecular mechanisms, *Pharmacology and Therapeutics*, **104**(3), pp. 163-172. DOI 10.1016/j.pharmthera.2004.08.006.

Ivakine, E.A., Acton, B.A., Mahadevan, V., Ormond, J., Tang, M., Pressey, J.C., Huang, M.Y., Ng, D., Delpire, E., Salter, M.W., Woodin, M.A. & McInnes, R.R. (2013), Neto2 is a KCC2 interacting protein required for neuronal $Cl^-$ regulation in hippocampal neurons, *Proceedings of the National Academy of Sciences of the United States*, **110**(9), pp. 3561. DOI 10.1073/pnas.1212907110.

Ko, S., Zhao, M., Toyoda, H., Qiu, C. & Zhuo, M. (2005), Altered Behavioral Responses to Noxious Stimuli and Fear in Glutamate Receptor 5 (GluR5)- or GluR6-Deficient Mice, *The Journal of Neuroscience*, **25**(4), pp. 977-984. DOI 10.1523/JNEUROSCI.4059-04.2005.

Lerma, J. (2003), Roles and rules of kainate receptors in synaptic transmission, *Nature Reviews Neuroscience*, **4**(6), pp. 481-495. DOI 10.1038/nrn1118.

Lomash, R.M, Sheng, N., Li, Y., Nicoll, R.A. & Roche, K.W. (2017) Phosphorylation of the kainate receptor (KAR) auxiliary subunit Neto2 at serine 409 regulates synaptic targeting of KAR subunit GluK1, *The Journal of Biological Chemistry,* **292**(37), pp. 15369–15377. DOI 10.1074/jbc.M117.787903

Maccarrone, G. & Filiou, M.D. (2015), Protein profiling and phosphoprotein analysis by isoelectric focusing, Proteomic Profiling: Methods and Protocols, *Methods in Molecular Biology,* New York: Springer Science+Business Media, **1295**, pp. 293-303. DOI 10.1007/978-1-4939-2550-6_22

Mahadevan, V., Dargaei, Z., Ivakine, E.A., Hartmann, A., Ng, D., Chevrier, J., Ormond, J., Nothwang, H.G., McInnes, R.R. & Woodin, M.A. (2015), Neto2-null mice have impaired GABAergic inhibition and are susceptible to seizures, *Frontiers in Cellular Neuroscience*, **9**(368). DOI 10.3389/fncel.2015.00368.

Marek, R., Xu, L., Sullivan, R.K.P. & Sah, P. (2018), Excitatory connections between the prelimbic and infralimbic medial prefrontal cortex show a role for the prelimbic cortex in fear extinction, *Nature Neuroscience*, **21**(5), pp. 654-658. DOI 10.1038/s41593-018-0137-x.

Maren, S. & Holmes, A. (2016), Stress and Fear Extinction, *Neuropsychopharmacology Reviews,* **41**(1), pp. 58-79. DOI 10.1038/npp.2015.180.

Mattheisen, M., Samuels, J.F., Wang, Y., Greenberg, B.D., Fyer, A.J., McCracken, J.T., Geller, D.A., Murphy, D.L., Knowles, J.A., Grados, M.A., Riddle, M.A., Rasmussen, S.A., McLaughlin, N.C., Nurmi, E.L., Askland, K.D., Qin, H., Cullen, B.A., Piacentini, J., Pauls, D.L., Bienvenu, O.J., Stewart, S.E., Liang, K., Goes, F.S., Maher, B., Pulver, A.E., Shugart, Y.Y., Valle, D., Lange, C. & Nestadt, G. (2015), Genome-wide association study in obsessive-compulsive disorder: results from the OCGAS, *Molecular psychiatry,* **20**(3), pp. 337-344. DOI 10.1038/mp.2014.43.

Meow (2012). Closed eppendorf tube with pellet clip art. Retrieved from http://www.clker.com/clipart-closed-eppendorf-tube-with-pellet.html (27.02.2018)

Michishita, M., Ikeda, T., Nakashiba, T., Ogawa, M., Tashiro, K., Honjo, T., Doi, K., Itohara, S. & Endo, S. (2004), Expression of Btcl2, a novel member of Btcl gene family, during development of the central nervous system, *Developmental Brain Research,* **153**(1), pp. 135-142. DOI 10.1016/j.devbrainres.2004.06.012.

Ng, D., Pitcher, G.M., Szilard, R.K., Sertié, A., Kanisek, M., Clapcote, S.J., Lipina, T., Kalia, L.V., Joo, D., McKerlie, C., Cortez, M., Roder, J.C., Salter, M.W. & McInnes, R.R. (2009), Neto1 is a novel CUB-domain NMDA receptor-interacting protein required for synaptic plasticity and learning, *PLoS biology*, **7**(2), e1000041, pp. 278-300. DOI 10.1371/journal.pbio.1000041.

Pahl, S., Tapken, D., Haering, S.C. & Hollmann, M. (2014), Trafficking of kainate receptors, *Membranes*, **4**(3), pp. 565-595. DOI 10.3390/membranes4030565

Palacios-Filardo, J., Aller, M.I. & Lerma, J. (2014), Synaptic Targeting of Kainate Receptors, *Cerebral cortex*, **26**(4), pp. 1464-1472. DOI 10.1093/cercor/bhu244.

Pinheiro, P. & Mulle, C. (2006), Kainate receptors, *Cell Tissue Res*, 326, pp. 457-482. DOI 10.1007/s00441-006-0265-6

Pray_For_Eliza (2011). Empty test tube clip art. Retrieved from http://www.clker.com/clipart-empty-test-tube.html (27.02.2018)

Shaltiel, G., Maeng, S., Malkesman, O., Pearson, B., Schloesser, R.J., Tragon, T., Rogawski, M., Gasior, M., Luckenbaugh, D., Chen, G. & Manji, H.K. (2008), Evidence for the involvement of the kainate receptor subunit GluR6 (GRIK2) in mediating behavioral displays related to behavioral symptoms of mania, *Molecular Psychiatry*, **13**(9), pp. 858-872. DOI 10.1038/mp.2008.20.

Sheng, N., Shi, Y.S., Lomash, R.M., Roche, K.W. & Nicoll, R.A. (2015), Neto auxiliary proteins control both the trafficking and biophysical properties of the kainate receptor GluK1, *eLife*, 4. DOI 10.7554/eLife.11682.

Sheng, N., Shi, Y.S. & Nicoll, R.A. (2017), Amino-terminal domains of kainate receptors determine the differential dependence on Neto auxiliary subunits for trafficking, *Proceedings of the National Academy of Sciences of the United States of America*, **114**(5), pp. 1159-1164. DOI 10.1073/pnas.1619253114.

Spijker, S. & Li, K.W. (2011), Dissection of Rodent Brain Regions, *Neuroproteomics*, Humana Press, pp. 23-26.

Strange, B.A., Witter, M.P., Lein, E.S. & Moser, E.I. (2014), Functional organization of the hippocampal longitudinal axis, *Nature reviews Neuroscience*, **15**(10), pp. 655-669. DOI 10.1038/nrn3785.

Straub, C. & Tomita, S. (2011), The regulation of glutamate receptor trafficking and function by TARPs and other transmembrane auxiliary subunits, *Current Opinion in Neurobiology,* **22**(3), pp. 488-495. DOI 10.1016/j.conb.2011.09.005.

Straub, C., Noam, Y., Nomura, T., Yamasaki, M., Yan, D., Fernandes, H.B., Zhang, P., Howe, J.R., Watanabe, M., Contractor, A. & Tomita, S. (2016), Distinct Subunit Domains Govern Synaptic Stability and Specificity of the Kainate Receptor, *Cell Reports,* **16**(2), pp. 531-544. DOI 10.1016/j.celrep.2016.05.093.

Tang, M., Pelkey, K.A., Ng, D., Ivakine, E., McBain, C.J., Salter, M.W. & McInnes, R.R. (2011), Neto1 is an auxiliary subunit of native synaptic kainate receptors, *The Journal of Neuroscience,* **31**(27), pp. 10009-10018. DOI 10.1523/JNEUROSCI.6617-10.2011.

Tang, M., Ivakine, E., Mahadevan, V., Salter, M.W. & McInnes, R.R. (2012) Neto2 interacts with the scaffolding protein GRIP and regulates synaptic abundance of kainate receptors, *PLoS One,* **7**(12): e51433. DOI 10.1371/journal.pone.0051433

Tomita, S. & Castillo, P.E. (2012), Neto1 and Neto2: auxiliary subunits that determine key properties of native kainate receptors, *The Journal of Physiology,* **590**(10), pp. 2217-2223. DOI 10.1113/jphysiol.2011.221101.

Tovote, P, Esposito, M.S., Botta, P., Chaudun, F., Fadok, J.P., Markovic, M., Wolff, S.B.E., Ramakrishnan, C., Fenno, L., Deisseroth, K., Herry, C., Arber, S. & Lüthi, A. (2016), Midbrain circuits for defensive behaviour, *Nature*, **534**(7606), pp. 206-212. DOI 10.1038/nature17996.

Watanabe-Iida, I., Konno, K., Akashi, K., Abe, M., Natsume, R., Watanabe, M. & Sakimura, K. (2016), Determination of kainate receptor subunit ratios in mouse brain using novel chimeric protein standards, *The Journal of Neurochemistry*, 136, pp. 295-305. DOI 10.1111/jnc.13384.

Wittchen, H.U., Jacobi, F., Rehm, J, Gustavsson, A., Svensson, M., Jönsson, B., Olesen, J., Allgulander, C., Alonso, J., Faravelli, C., Fratiglioni, L., Jennum, P., Lieb, R., Maercker, A., van Os, J., Preisig, M., Salvador-Carulla, L., Simon, R., Steinhausen, H.C. (2011), The size and burden of mental disorders and other disorders of the brain in Europe 2010, *European Neuropsychopharmacology*, **21**(9), pp. 655-679. DOI 10.1016/j.euroneuro.2011.07.018.

Wu, LJ., Ko, S.W., Toyoda, H., Zhao, MG., Xu, H., Vadakkan, K.I., Ren, M., Knifed, E., Shum, F., Quan, J., Zhang, XH. & Zhou, Min (2007), Increased Anxiety-like behavior and enhanced synaptic efficacy in amygdala of GluR5 knockout mice, *PLoS One,* **2**(1): e167. DOI10.1371/journal.pone.0000167

Wyeth, M.S., Pelkey, K.A., Yuan, X., Vargish, G., Johnston, A.D., Hunt, S., Fang, C., Abebe, D., Mahadevan, V., Fisahn, A., Salter, M.W., McInnes, R.R., Chittajallu, R. & McBain, C.J. (2017), Neto Auxiliary Subunits Regulate Interneuron Somatodendritic and Presynaptic Kainate Receptors to Control Network Inhibition, *Cell Reports*, **20**(9), pp. 2156-2168. DOI 10.1016/j.celrep.2017.08.017.

Wyeth, M.S., Pelkey, K.A., Petralia, R.S., Salter, M.W., McInnes, R.R. & McBain, C.J. (2014), Neto auxiliary protein interactions regulate kainate and NMDA receptor subunit localization at mossy fiber-CA3 pyramidal cell synapses, *The Journal of Neuroscience*, **34**(2), pp. 622-628. DOI 10.1523/JNEUROSCI.3098-13.2014.

Zhang, W., St-Gelais, F., Grabner, C.P., Trinidad, J.C., Sumioka, A., Morimoto-Tomita, M., Kim, K.S., Straub, C., Burlingame, A.L., Howe, J.R. & Tomita, S. (2009), A Transmembrane Accessory Subunit that Modulates Kainate-Type Glutamate Receptors, *Neuron,* **61**(3), pp. 385-396. DOI 10.1016/j.neuron.2008.12.014.

Zhuo, M. (2017), Cortical kainate receptors and behavioral anxiety, *Molecular Brain,* 10. DOI 10.1186/s13041-017-0297-8.

# 6. Supplementary material

## 6.1. Appendix 1 - Synaptic protein enrichment blots

A

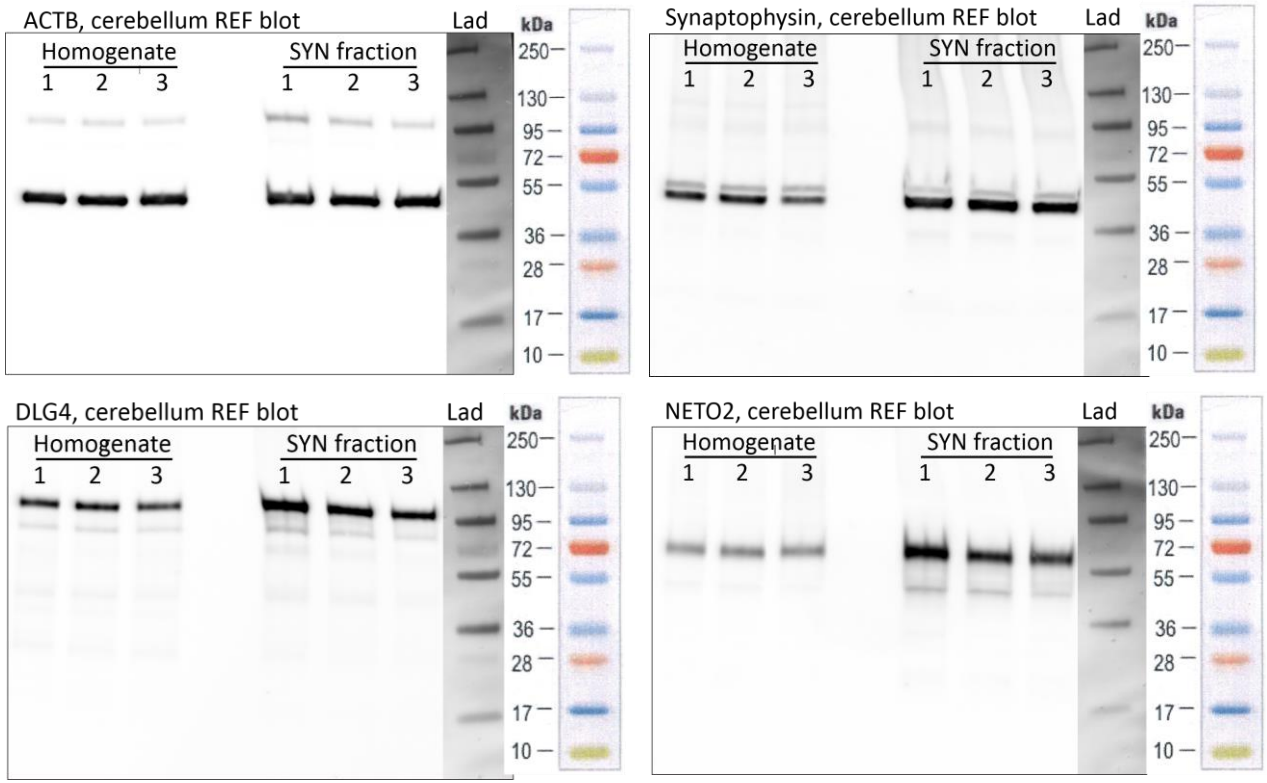

B

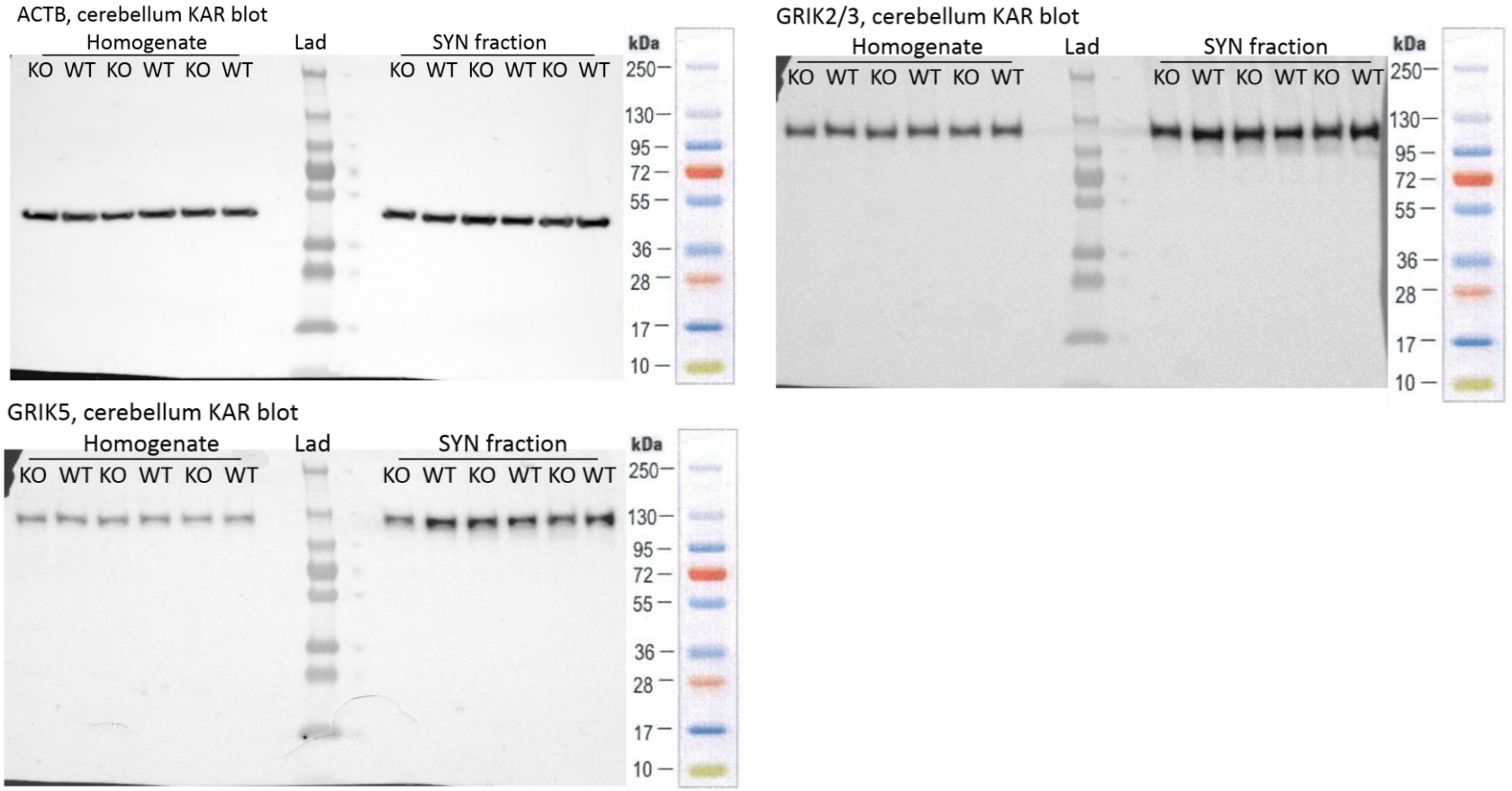


**Appendix 1. Full synaptic protein enrichment blots. A.** Reference (REF) western blots of homogenate (H) and SYN fractions from male WT cerebella (samples 1-3), using antibodies for ACTB, DLG4, synaptophysin (SYP) and NETO2 (*n* = 3 mice / blot). Respective image of ladder superimposed on respective blot. **B.** KAR western blots of H and SYN fractions from male WT (*n* = 3 mice / blot) and KO cerebella (*n* = 3 mice / blot), using antibodies for ACTB, GRIK2/3 and GRIK5. Schematic ladder adapted from manufacturer's product information booklet (Thermo Fisher Scientific, Waltham, MA, USA). Lad: Prestained Protein Ladder.

## 6.2. Appendix 2 - Cerebellum triplicate SYN blots

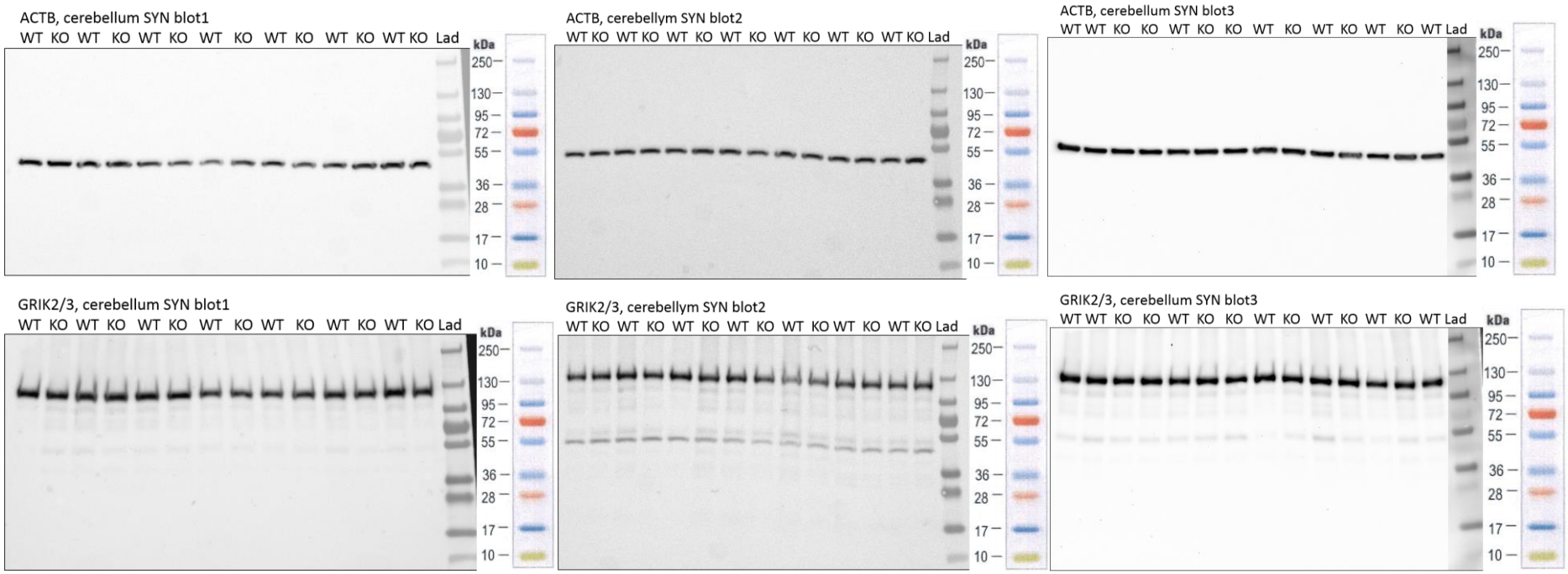

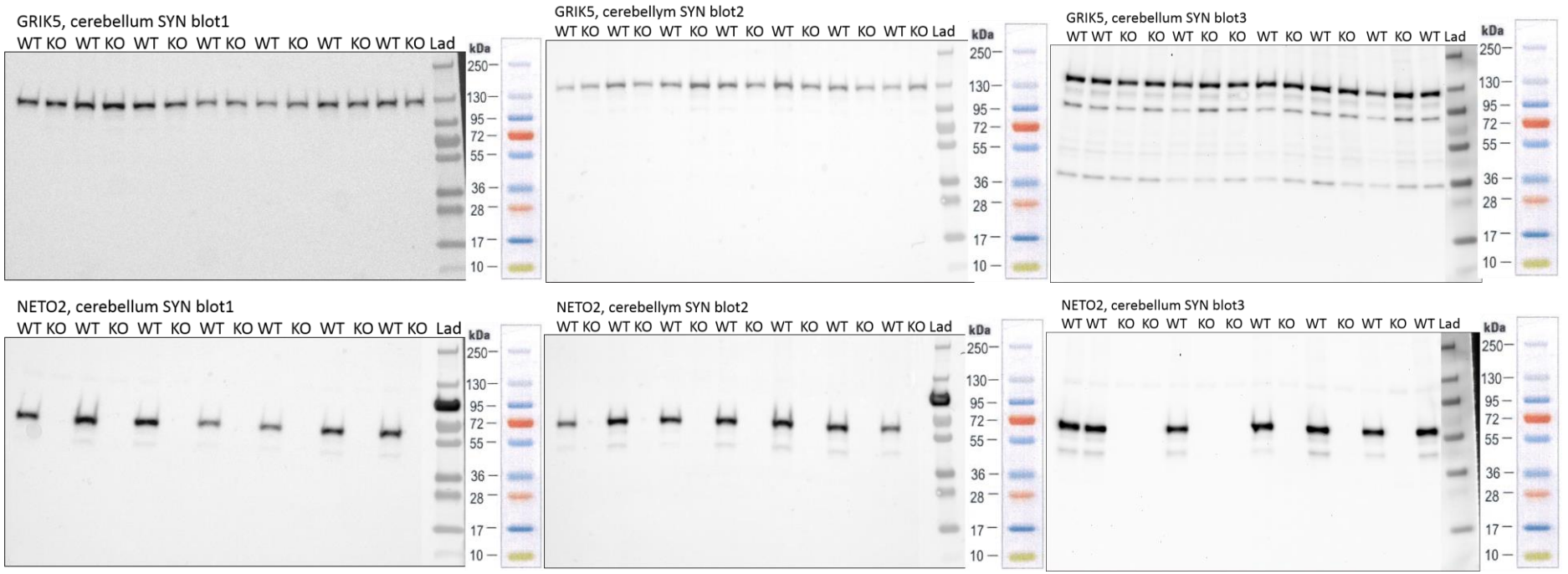


**Appendix 2. Full cerebellum triplicate SYN blots.** Western blots of cerebellar SYN fractions from *Neto2* WT (*n* = 7 / blot) and KO (*n* = 7 / blot) mice, using antibodies for ACTB, GRIK2/3, GRIK5 and NETO2 three times each. Respective image of ladder in third blot superimposed on respective blot. Schematic ladder adapted from manufacturer's product information booklet (Thermo Fisher Scientific, Waltham, MA, USA). Lad: Prestained Protein Ladder.

## 6.3. Appendix 3 - vHPC triplicate SYN blots

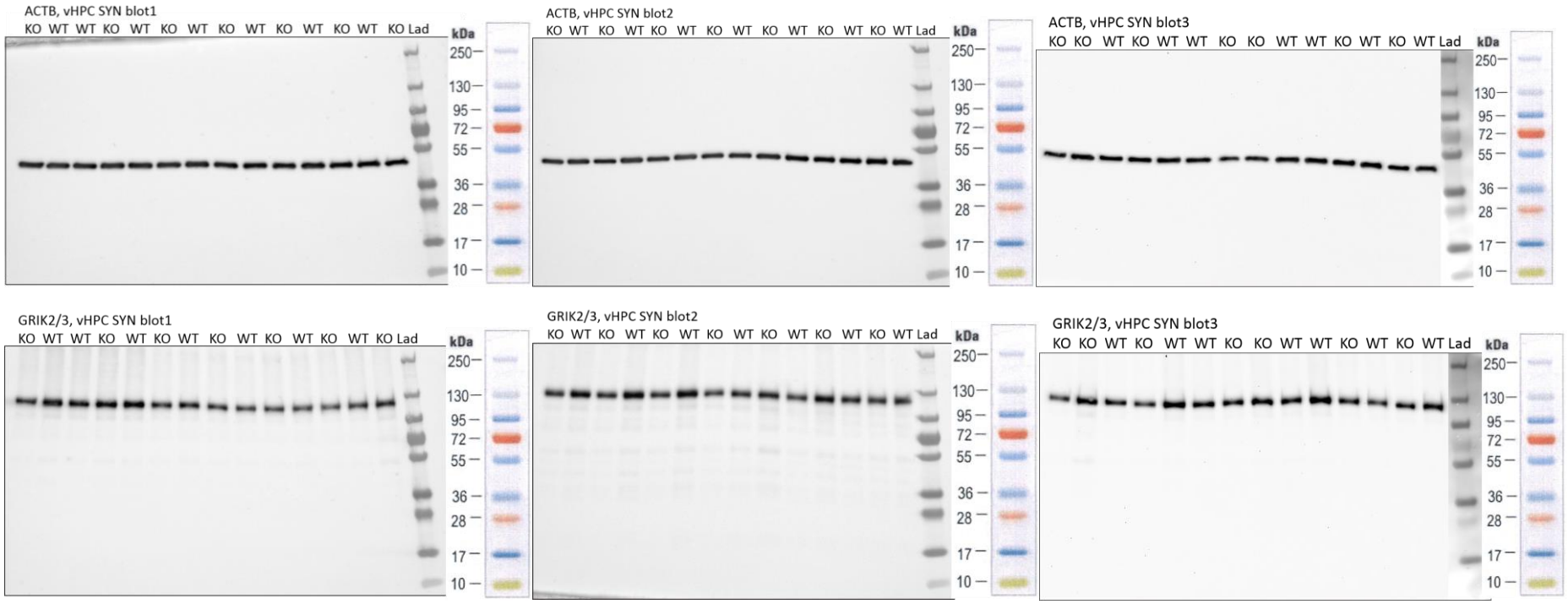

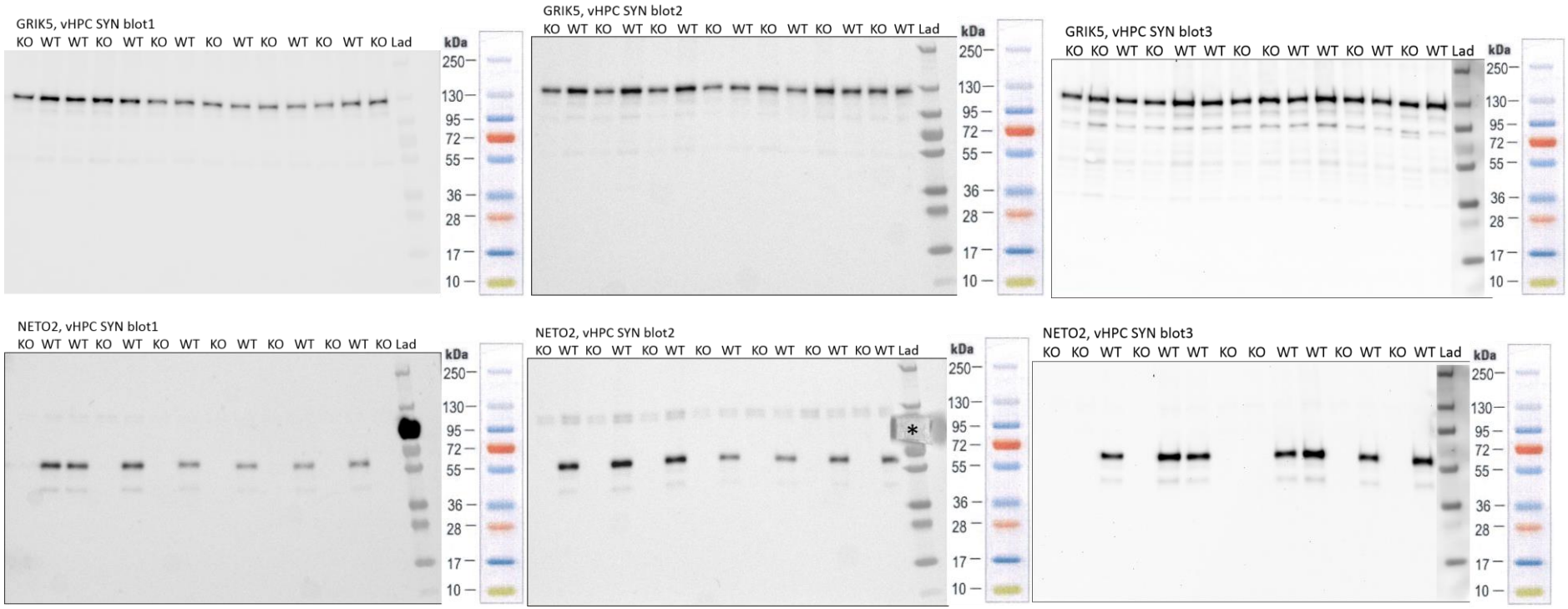


**Appendix 3. Full vHPC triplicate SYN blots.** Western blots of ventral hippocampal (vHPC) SYN fractions from *Neto2* WT (*n* = 7 / blot) and KO (*n* = 7 / blot) mice**,** using antibodies for ACTB, GRIK2/3, GRIK5 and NETO2. Ladder images in third blots are superimposed on their respective blot. Schematic ladder adapted from manufacturer's product information booklet (Thermo Fisher Scientific, Waltham, MA, USA). Lad: Prestained Protein Ladder. *A piece of paper towel covering the 95 kDa band on the ladder as its strong signal interfered with the NETO2 signal.

## 6.4. Appendix 4 - Amygdala triplicate SYN blots

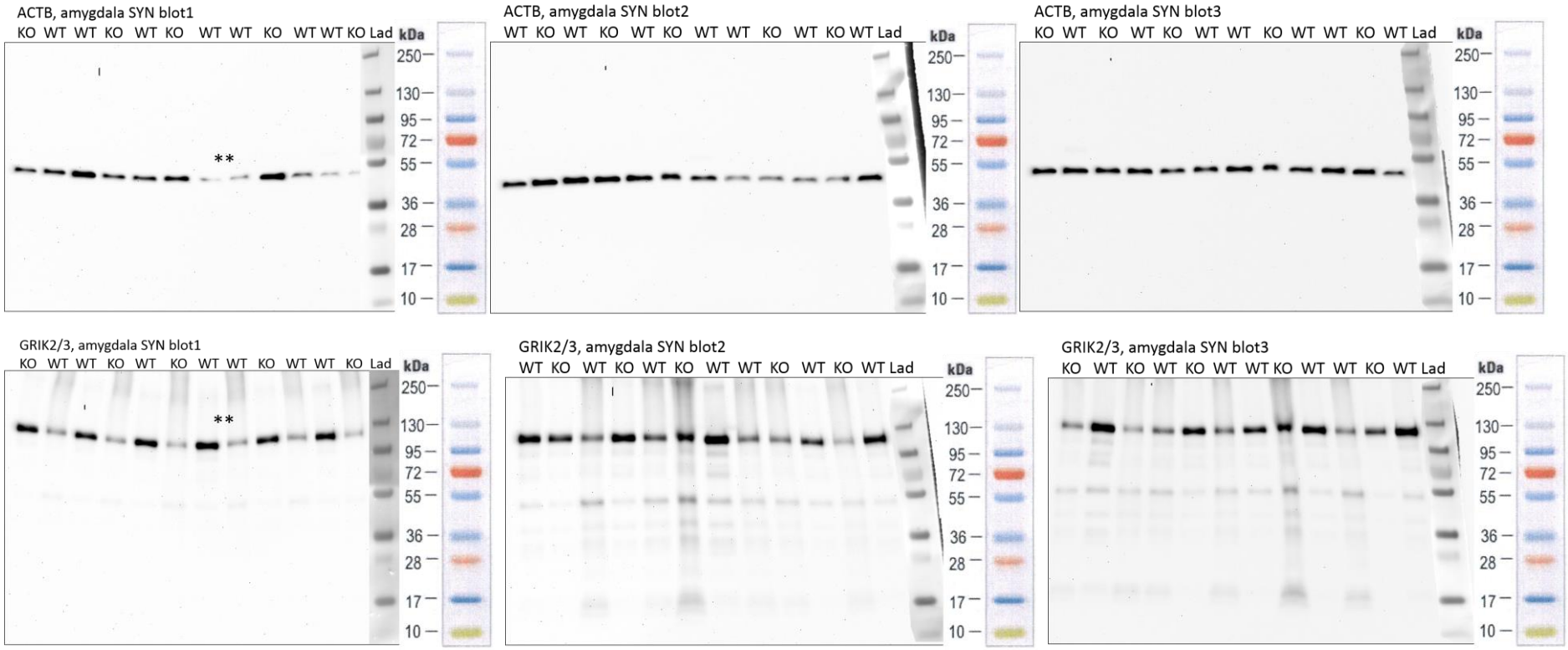

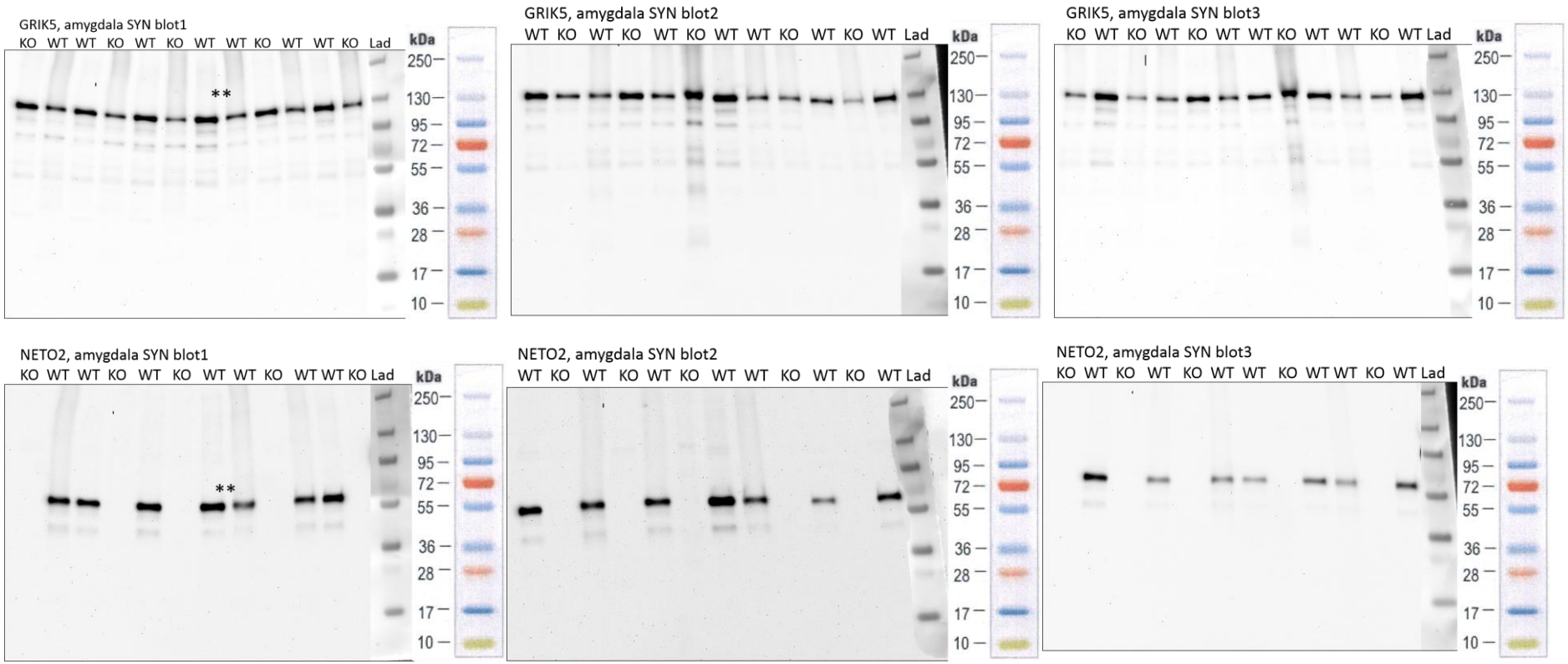


**Appendix 4. Full amygdala triplicate SYN blots.** Western blots of amygdalar SYN fractions from *Neto2* WT (*n* = 7 / blot) and KO (*n* = 5 / blot) mice**,** using antibodies for ACTB, GRIK2/3, GRIK5 and NETO2. Ladder images are superimposed on their respective blot. Schematic ladder adapted from manufacturer's product information booklet (Thermo Fisher Scientific, Waltham, MA, USA). Lad: Prestained Protein Ladder. **Two WT samples (one male, one female) in the first round were removed from analysis due to a technical issue.

## 6.5. Appendix 5 - mPFC triplicate SYN blots

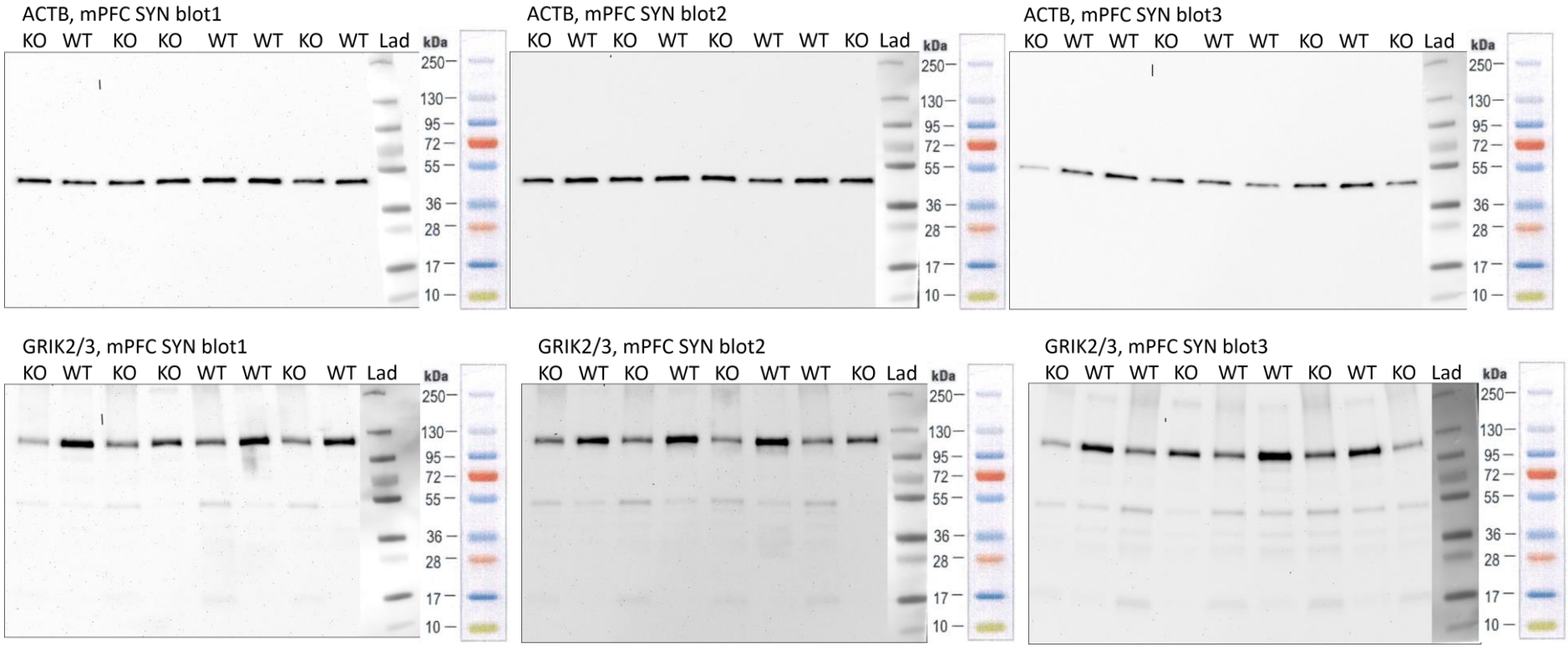

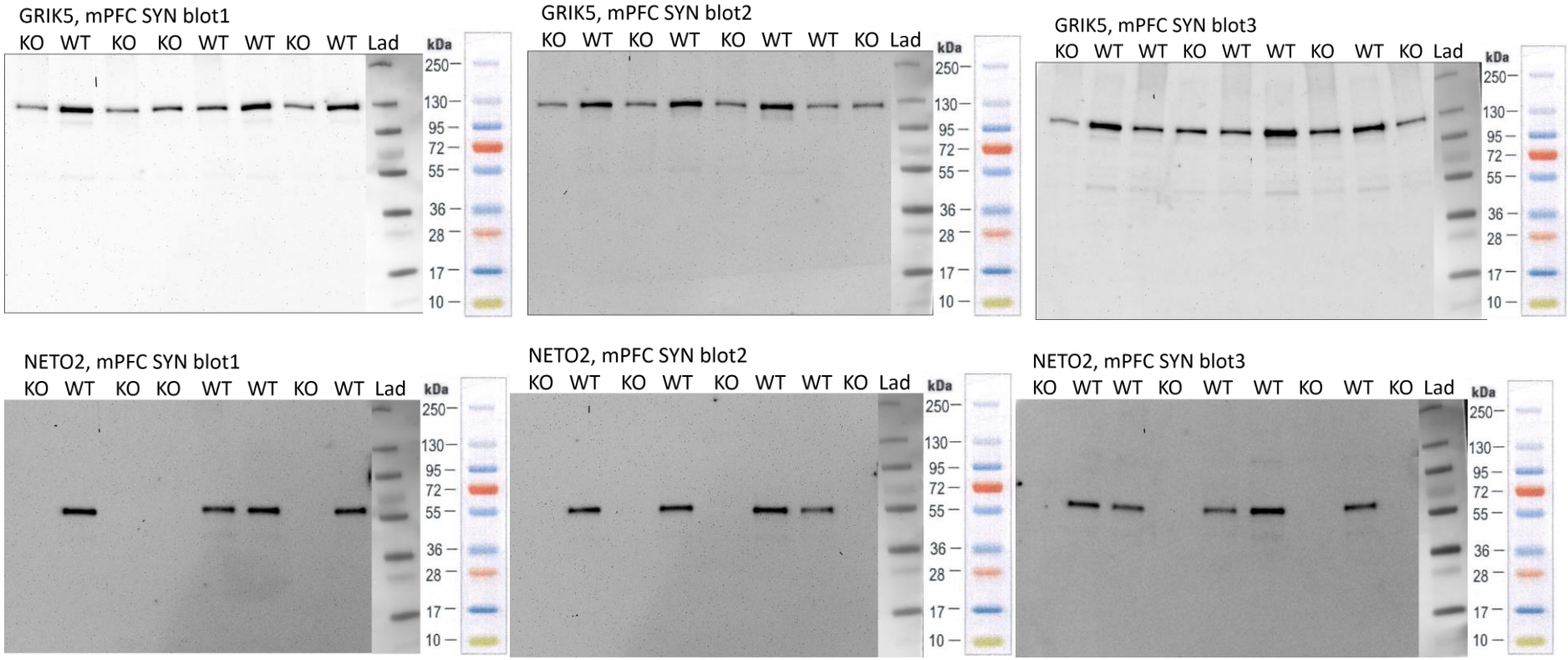


**Appendix 5. Full mPFC triplicate SYN blots.** Western blots of medial prefrontal cortical (mPFC) SYN fractions from *Neto2* WT (*n* = 4-5 / blot) and KO (*n* = 4 / blot) mice**,** using antibodies for ACTB, GRIK2/3, GRIK5 and NETO2. Ladder images superimposed on their respective blot. One male WT sample had a volume that was enough only for one round. It was used in the third round. Schematic ladder adapted from manufacturer's product information booklet (Thermo Fisher Scientific, Waltham, MA, USA). Lad: Prestained Protein Ladder.